

Progress in integrated die-casting technology for aluminum alloys

Yisheng Miao¹, Zhongyao Li², Ye Tian¹, Qinghuai Hou¹, Shihao Wang², Junsheng Wang^{1,2,3*}

- 1. School of Materials Science and Engineering, Beijing Institute of Technology, Beijing, 100081, China;
 - 2. School of Mechanical Engineering, Beijing Institute of Technology, Beijing 100081, China;
 - 3. School of Multidisciplinary Science, Beijing Institute of Technology, Beijing, 100081, China.
 - * Corresponding author. Tel.: +86 010 68915043. E-mail: junsheng.wang@bit.edu.cn (J.S. Wang)

Abstract: Due to their low density, high specific strength, good toughness, and corrosion resistance, aluminum alloys have become core materials for lightweight structural components, finding wide application in the aerospace and automotive industries. In recent years, non-heat-treatable integrated die-casting technology has developed rapidly in the field of new energy vehicle manufacturing, driving profound transformations in the automotive sector by enhancing part performance, improving production efficiency, and reducing manufacturing costs. This paper systematically reviews the research progress on non-heat-treatable aluminum alloys for die casting, with particular emphasis on the alloy design and microstructure characteristics. The mechanisms underlying the formation of common defects during die-casting, corresponding process optimization strategies, and their effects on mechanical properties are discussed in details. Finally, the technical advantages, typical applications, existing challenges, and future development trends of integrated die- casting technology are summarized.

Keywords: Non-heat-treatable aluminum alloys; Integrated die casting; Mechanical properties; Micropores; Numerical simulatio

1 Introduction

In recent years, to address the global shortage of fossil energy, traditional high-energy-consumption industries have been compelled to transition toward decarbonization, with energy conservation and emission reduction playing a pivotal role.[1] Research data from the automotive industry indicates that for every 30% reduction in vehicle weight, fuel efficiency can be improved by 20%-24%, and carbon dioxide emissions can be reduced by 20%. This demonstrates that vehicle lightweighting has become a crucial strategy for energy conservation and emission reduction in the transportation sector^[2]. Aluminum and its alloys, owing to their low density, high specific strength, and excellent recyclability, have emerged ideal materials automotive lightweighting^[3]. At present, die casting is the predominant manufacturing process for aluminum automotive components. Die casting refers to the process in which molten or semi-molten metal is injected into a mold cavity under high pressure and high speed, followed by solidification under pressure to form the final casting^{[4],[5]}. However, traditional die-casting techniques are incapable of producing large structural components, such as underbody panels and longitudinal beams, as integrated parts. Instead, smaller components must first be cast individually and then assembled, which often results in poor surface quality, reduced impact resistance, and lower mechanical strength. These shortcomings introduce potential safety risks. In 2019, Tesla introduced integrated die-casting technology for the Model Y chassis, replacing approximately 370 individual components with just 2-3 large castings. This advancement marked a significant breakthrough in die-casting technology by enabling the one-shot forming of large structural parts. The implementation of this technology resulted in a 30% reduction in vehicle body weight, a 40% decrease in manufacturing costs, and a substantial improvement in overall safety performance^[6]. Tesla's successful application has drawn unprecedented attention to integrated die casting technology across the automotive industry. In particular, this technology is undergoing rapid development in China, with continuous progress being achieved in both academic research and industrial implementation. Several major domestic manufacturers, including NIO, ZEEKR, and Xiaomi Auto, are actively employing this technology to produce ultra-large components such as front cabins and rear underbodies. However, several critical challenges remain. Owing to the presence of significant residual stress within large integrated die cast aluminum components such as rear underbodies these structures are highly susceptible to deformation during heat treatment. The thermal expansion effect may result in severe distortion and dimensional deviation which renders conventional heat treatment strengthening unsuitable for such large scale castings. In response to these issues the development of non-heat-treatable die cast aluminum alloys and their application in integrated die casting has gradually become a major focus of current research^{[7]–[9]}. In addition, during the melting stage, undissolved gases often remain trapped within the interdendritic regions of the molten metal, which commonly leads to the formation of gas pores in die-cast components^{[10],[11]}. The presence of such defects severely compromises the mechanical integrity of the casting, rendering it unsuitable for load-bearing structural applications and limiting its performance under elevated temperature conditions.

Therefore, an overview of recent progress in the compositional design of Al-Si and Al-Mg alloys is first provided, focusing on the underlying concepts and strategic approaches. To address the typical casting defects commonly observed in integrated die casting, including gas pores, shrinkage pores, and hot cracking, this paper provides a detailed analysis of their primary types, morphological characteristics, and formation mechanisms. In addition, effective approaches for controlling these defects and improving performance through the optimization of process parameters are discussed. Furthermore, this paper summarizes the quantitative relationships between micropore characteristics such as size, morphology, distribution, and location and their effects on mechanical properties. These findings provide theoretical support for fatigue life prediction and structural design optimization. In conclusion, by reviewing the practical applications of integrated die casting technology among leading domestic automotive manufacturers, this paper evaluates its advantages and technical challenges in the production of new energy vehicles and provides perspectives on future development trends and research directions.

2 Research progress of aluminum alloy systems for integrated die casting

The intrinsic properties of cast aluminum alloys largely determine their upper-limit applicability in structural components. With the rapid development of new energy vehicles, automotive structural parts are evolving toward highly integrated, lightweight, and efficient design and manufacturing. Representative examples include the one-piece hot-stamped door ring, the integrated die-cast body, and the integrated die-cast subframe^[12]. For large-sized integrated die-cast aluminum components, the alloy system must meet several critical requirements^[13]. (1) Excellent fluidity is essential for achieving complete mold filling and ensuring high surface quality. (2) Sufficient mechanical strength at both room and elevated temperatures is required to meet the demands of large, complex, and thin-walled structural parts. (3) A narrow solidification temperature range helps to reduce shrinkage-related defects and improve the casting quality. (4) Low reactivity between the alloy and the die material reduces the risk of die sticking or soldering during casting. (5) Superior corrosion resistance and structural integrity are necessary for reliable operation under harsh environmental conditions^[14]. Among the various cast aluminum alloy systems, Al-Si and Al-Mg alloys have emerged as the primary focus of current research and the mainstream choice for integrated die casting applications due to their excellent castability and well-balanced mechanical properties.

2.1 Al - Si alloy

2.1.1 Composition design

The Al-Si die-cast aluminum alloy system has become the primary focus in integrated die casting applications due to its excellent fluidity. Typically, the composition of die-cast aluminum alloys have a significant influence on the mechanical performance of structural components^[15]. The selection and proportion of alloying elements are critical for promoting the formation of sufficient strengthening phases while maintaining the desired level of fluidity^[16]. As the primary alloying element in Al–Si alloy systems, Si is typically present in the range of 4 to 11.5 wt.%^[17]. The addition of Si significantly enhances melt fluidity, mitigates shrinkage pores, and reduces the tendency for hot cracking. Moreover, it contributes to an improvement in tensile strength to a certain extent. During solidification, the formation of eutectic strengthening phases further imparts superior mechanical properties to the alloy. However, owing to the relatively coarse eutectic structure of Al-Si alloys, alloying



elements such as Cu, Mg, Mn, Sr, and rare earth elements are commonly added to further enhance their overall properties. The chemical compositions and mechanical properties of newly developed Al–Si die-cast alloys, designed for enhanced strength, toughness, and ductility, are presented in Tables 1 and 2, respectively.

In Al-Si alloys, the Fe element is primarily added to prevent die soldering. However, its content is typically restricted to below 0.5 wt.% as excessive Fe may result in the formation of brittle intermetallic phases that significantly degrade the mechanical properties of the alloy. In Al-Si alloys, Fe commonly exists in two typical phases. One is in the form of plate-like or needle-like structures, primarily located at grain boundaries, with the chemical formula β-Al₅FeSi, as shown in Fig. 1(c)^[18]. This needle-like phase can split the matrix and significantly reduce the alloy's toughness, making it a detrimental phase. The other phase appears in a Chinese-script or fishbone morphology, with the chemical formula α-Al₈Fe₂Si, as shown in Fig. 1(d). It contributes to the increased strength and hardness of the alloy. An increase in Fe content from 0.8 wt.% to 1.0 wt.% in Al-Si alloys has been shown to significantly reduce both tensile strength and ductility, with values dropping from 230 MPa to 205 MPa and from 1.2% to 0.79%, respectively^[19]. To mitigate the detrimental effects associated with Fe, some researchers have attempted to partially substitute Fe with Mn. The addition of Mn promotes the formation of intermetallic phases such as Al₆Mn or Al₁₅(Mn,Fe)₃Si₂, which helps suppress the formation of brittle phases commonly generated under high Fe concentrations. Consequently, the mechanical properties of die-cast Al-Si alloys can be effectively improved^[20]. To enhance the mechanical properties, Mg is commonly added to Al-Si alloys. The incorporation of Mg leads to the formation of Mg2Si strengthening phases. It has been reported that each 0.1 wt.% increase in Mg content can improve the yield strength by approximately 10 MPa. However, this enhancement is accompanied by a reduction in ductility. Therefore, the Mg content is typically limited to below 0.5 wt.%^[21]. During T5 or T6 heat treatments, the metastable strengthening phase Mg₅Si₄Al₂ precipitate, thereby enhancing the alloy's strength. For example, in the Silafont 36 alloy (Rheinfelden Alloys), T5 treatment can increase the yield strength by approximately 100 MPa compared to the as-cast condition. After T6 treatment, the yield strength can reach ~240 MPa, while the ultimate tensile strength can increase to 310 MPa (see Table2). Similarly, T5 heat treatment is also applicable to the Aural alloys (Magna) with varying Si contents. Among them, Aural 2 exhibits the highest strength, reaching up to approximately 340 MPa, while Aural 5 demonstrates a favorable combination of strength and ductility, with elongation ranging from 6% to 12%^[22]. Similar to Mg, Cu enhances the strength and hardness of Al–Si alloys primarily through the formation of Al2Cu precipitates. However, excessive Cu content can significantly deteriorate the corrosion resistance of the alloy^[23]. As a surface-active element, Sr can fundamentally alter the behavior of intermetallic phases. Therefore, Sr is commonly used for alloy modification treatments to effectively improve the ductility, machinability, and overall quality of Al alloys. Sr exerts a spheroidizing and modifying effect on the eutectic Si phase, effectively hindering grain boundary migration and dislocation slip. As a result, the strength of the alloy is enhanced, along with improved fracture toughness, thermal expansion behavior, and workability. In addition, the addition of 0.015-0.03 wt.% Sr to extrusion aluminum alloys can promote the transformation of the β-AlFeSi phase into the α-AlFeSi phase, thereby improving the mechanical properties of the material and reducing surface roughness of the final product^[24]. Li et al. systematically investigated the effects of Sr on the morphology and size of Fe-rich phases using X-ray computed tomography (XCT). Their results revealed that Sr addition reduces both the size and volume fraction of Fe-rich phases in the as-cast alloy, and the underlying mechanism was further elucidated at the atomic scale^[25]. Ti and B are commonly added to Al-Si alloys as grain refiners. During solidification, they promote the formation of TiB2 particles, which serve as potent nucleation sites, thereby refining the grain structure and enhancing the alloy's strength, toughness, and ductility. Hu et al. investigated a high-pressure die-cast, non-heat-treatable Al9Si0.6Mn alloy and found that the addition of 1 wt.% and 2 wt.% TiB2 significantly refined the grain structure, with the average grain size decreasing from 17.1 µm to 13.1 µm and 9.3µm, respectively^[26]. Correspondingly, the yield strength and ultimate tensile strength increased by 9.7 MPa and 11.2 MPa, while the elongation slightly decreased from 9.5% to 8.8% and 8.3%, respectively, as shown in Fig. 2.

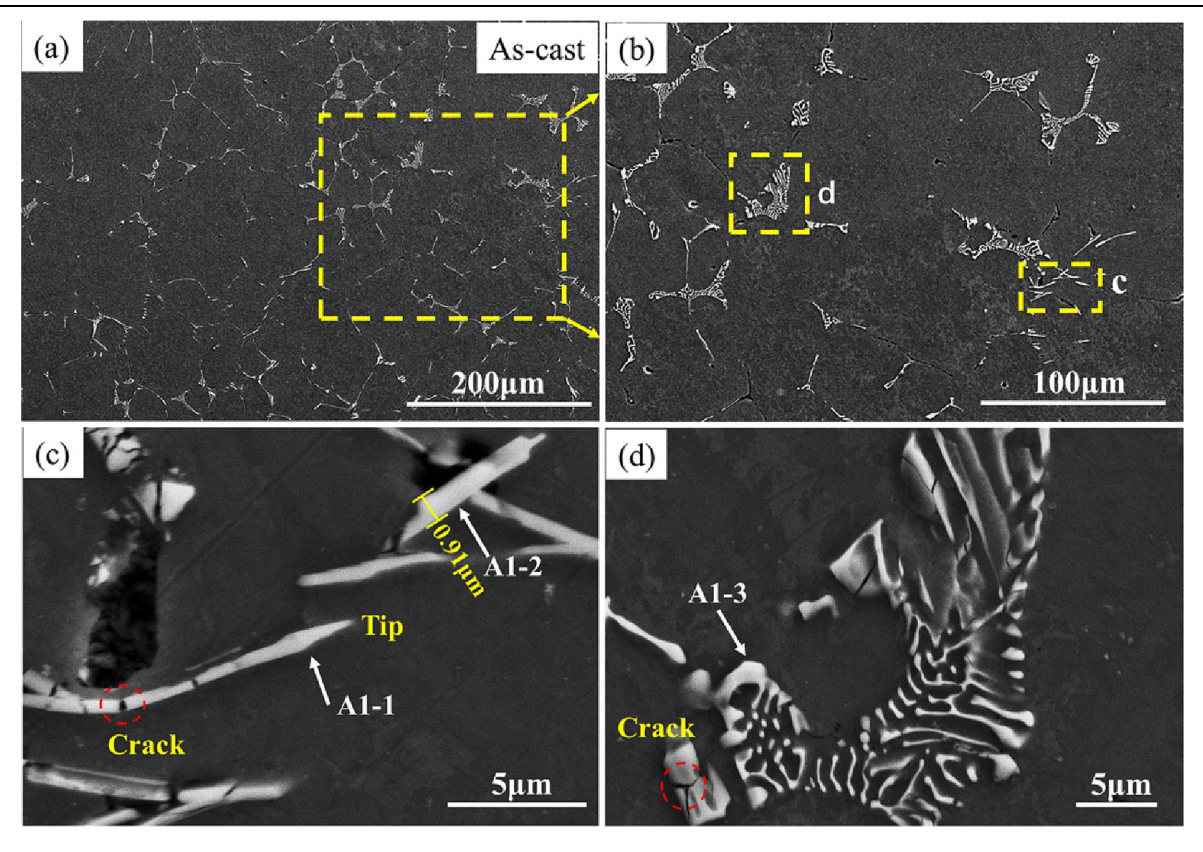


Fig.1 Microstructure of as-cast Al–Si alloy: (a) low-magnification optical micrograph; (b) enlarged view of the selected region in (a); (c) typical morphology of the β-Al₅ FeSi Fe-rich phase; (d) typical morphology of the α-Al₅Fe₂Si phase^[18].

Table1. Elemental content of Al-Si series alloys

	Al–Si	Element content(wt%)													
Companies	alloy system	Si	Fe	Cu	Mn	Mg	Zn	Ti	Sr	Other	Refs				
	Silafont 36	9.5–11. 5	< 0.15	< 0.03	< 0.8	0.1-0.5		0.04-0							
Rheinfelde n	Silafont-	8.5-10.0	<0.15	0.1-0.4	0.4-0.8	0.3-0.4	0.1-0.	< 0.15		Zr,Mo	[22]				
	Castasil 37	8.5–10. 5	< 0.15	< 0.05	0.35–0. 6	< 0.06	0.07	< 0.2	< 0.2 0.006–0. 025						
Magna	Aural 2	9.5–11. 5	0.15–0. 2	< 0.03	0.45–0. 55	0.27–0. 33		< 0.08	0.01–0.0 16	< 0.03	[27]				
	Aural 3	9.5–11. 5	0.15–0. 2	< 0.03	0.45–0. 55	0.4-0.6		< 0.08	0.01–0.1 6	< 0.03					
	Aural 4	4.0–4.5	0.15–0. 2	< 0.03	0.45–0. 8	0.4-0.5		< 0.08	0.004–0. 007	< 0.03	[6],[22], [28]				
	Aural 5	6.5–9.5	0.15–0. 2	< 0.03	0.3-0.6	0.1-0.6		< 0.08	0.03						
Mercury Castings	Mercall oy A368	8.5–9.5	0.25	0.25	0.25–0. 35	0.1-0.3	0.1	0.2	0.05–0.0 7	< 0.15	[6],[13],				
Mercury Castings	Mercall oy A367	8.5–9.5	0.25	0.25	0.25–0. 35	0.3-0.5	0.1	0.2	0.05–0.0 7	< 0.15	[22]				

5

FAW

	AFU									Part 2: 1	von-r erro	ous Alloy
	.1	EZCast 370	6.0–9.0	< 0.2		0.1-0.8	0.15–0. 8		< 0.2	0.01–0.0 25	< 0.05	[29]
	Alcoa	C611	6.0-9.0	< 0.15		0.4-0.8	0.15-0. 30		<0.1	0.01-0.0	< 0.05	[27]
Tesla	Tesla Alloy 1	6.5-7.5	0.4	0.4-0.8	0.3-0.7	0.1-0.4		< 0.15	0.01-0.0	V, Cr		
	Tesla Alloy 2	6—11	0.5	0.3-0.8	0.35-0. 8	0.15-0. 4		< 0.15	0.015-0. 05	V, Cr	[30]	
		Tesla Alloy 3	6—11	0.5	0.3-0.8	0.35-0. 8	0.1-0.4		< 0.15	0.015-0. 05	V, Cr	
	LIZHONG GROUP	LDHM- 02	9.1~10	0.15	0.03	$0.35 \sim$ 0.6	0.06	0.05	$0.06 \sim 0.15$	$0.015 \sim 0.025$	Mo, Zr	[31]
	Chinalc	ZL	7.5-9.5			0.4-0.8	0-0.4		0.03-0. 1	0.005-0. 025	Ni, Gr, Zr	[32]
	Tsinghua University	THAS-1	8-11	0.2		0.4-0.8				0.01-0.0	V, Zr	[33]
	Shanghai Jiao Tong University	JDA1	8-10	0.2	0.05-0. 5	0.5-0.8	0.1-0.5		0.05-0. 2	0.01-0.0	V, RE	[34]
	Guangdon	HT11	7-10	0.1-0.2	0.05	0.3-0.7		0.07	0.03-0. 2	0.015-0. 03	V	[35]
	g Hongtu	HT22	7-10	0.1-0.2	0.05	0.3-0.7	0.2-0.3	0.07	0.03-0. 2	0.015-0. 03	V	
	Xiaomi	Tiantans	6.5-8.3	0.09-0. 25	0.25-0. 5	0.5-0.8	0.2-0.4	0.25	0.05-0. 2	0.02-0.0	Zr, Hf, Re	[36]
	CHINA	-	6-8	0.5-0.6	0.6-0.9	0.6-0.8	0.3-0.4		0.1-0.2	0.02-0.0		[37]

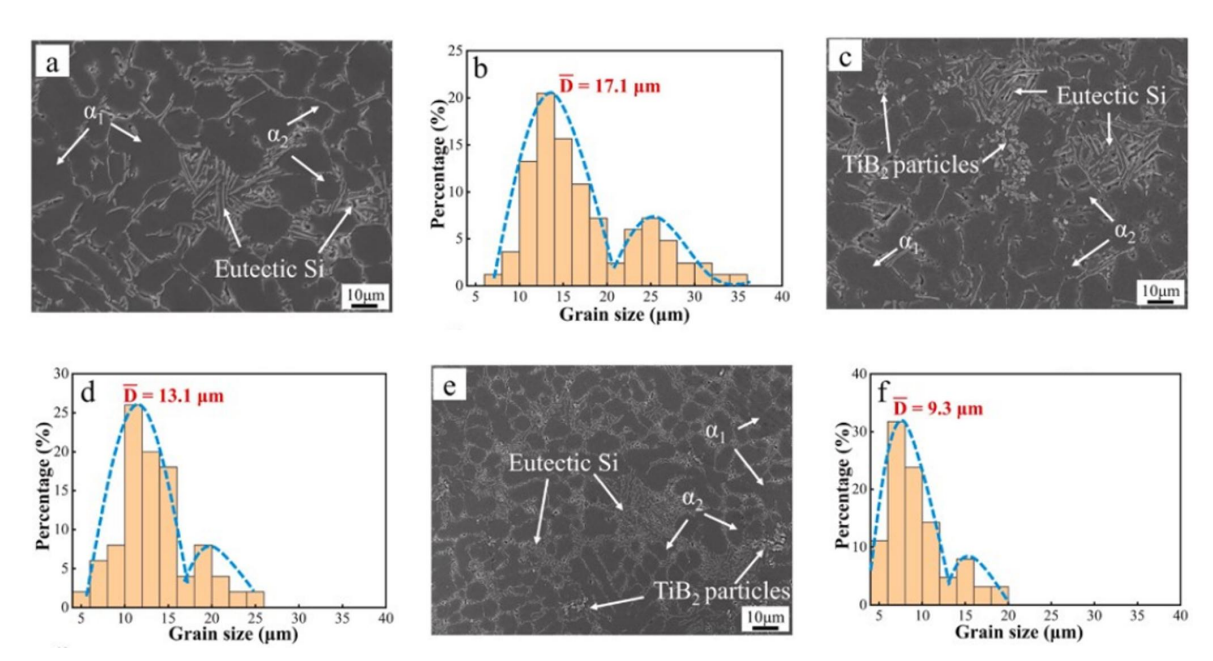


Fig. 2. SEM images and grain size statistics: (a–b) Al9Si0.6Mn alloy; (c–d) Al9Si0.6Mn-1TiB₂ alloy; (e–f) Al9Si0.6Mn–2TiB₂ alloy^[26]

2.1.2 Recent advances in domestic and international research At present, numerous institutions both in China and abroad have independently developed their die-cast Research and development aluminum alloys. non-heat-treatable die-cast alloys was first initiated overseas. C611, part of the EZCast alloy series developed by Alcoa for large structural castings, is a representative heat-treatment-free alloy. Its chemical composition includes 0.01-0.03 wt.% Sr, which contributes to its excellent high-temperature fluidity and good demoldability. The alloy exhibits a tensile strength of 268 MPa, a yield strength of 123 MPa, and an elongation of 16.2%, outperforming Castasil 37 in overall performance. At present, the C611 aluminum alloy has been applied in the manufacturing of all-aluminum bodies for vehicles such as the Audi A8 and Ferrari 360 Modena^[38]. Similar to the C611 non-heat-treatable structural die-cast aluminum alloys, Aural 6 and Aural 5, have been developed by Magna in Canada. Among them, Aural 6 is commonly used for producing self-piercing riveted (SPR) structural components in car bodies due to its excellent ductility and natural ageing stability after casting and before paint baking. Other alloys with comparable performance to the Aural series include the EZCast series developed by Alcoa and the Mercalloy 368 and 367 alloys^{[4],[6],[22]}. Castasil 37 is a non-heat-treatable Al-Si die-cast aluminum alloy developed by Rheinfelden Alloys in Germany. When the Mg content is 0.06 wt%, the alloy exhibits a tensile strength of 230 MPa, a yield strength of 120 MPa, and an elongation exceeding 10%, as shown in Table 2. To achieve a synergistic improvement in strength and toughness, Jason introduced a series of newly developed alloys by Tesla (Tesla alloy 1, Tesla alloy 2, and Tesla alloy 3) in a recent patent. These alloys enhance strength without significantly compromising ductility by precisely controlling the Cu/Mg ratio, which promotes the precipitation of the AlCuMgSi phase instead of the conventional Mg2Si and Al2Cu phases. In addition, Sr is added to modify the morphology of the Si phase, and V is introduced to promote the formation of spherical AlFeSi(Mn+V) phases while reducing the formation of plate-like Fe-rich phases. Both modifications contribute to improved toughness. The final as-cast alloy, designed for large structural castings, exhibits a yield strength of at least approximately 130 MPa and a bending angle of at least approximately 20 degrees at a section thickness of 3 mm, and has been successfully applied in the Tesla Model Y^[30].

Table2. Mechanical properties of typical high-strength and high-toughness aluminum alloys

Grades	Temper	YS	UTS	EI	Alloy	Grades	Tompor	YS	UTS	EI	Alloy
Grades	remper	(MPa)	(Mpa)	(%)	system	Grades	Temper	(MPa)	(Mpa)	(%)	system
Silafont 36	F	120-150	250-290	5—11	Al-Si		F	105-140	250-280	7.5–13	Al-Si
	T5	157– 212	290–316	4.5–8.9	Al-Si	EZCast 370	Т6	135–250	195–300	7–16	Al-Si
	Т6	240– 250	300–310	7.1–10	Al-Si	Tesla Alloy 1	F	130			Al-Si
Silafont-	F	140-160	270-300	4-7	Al-Si	Tesla Alloy 2	F	130			Al-Si
Castasil 37	F	120– 150	230–300	10–14	Al-Si	Tesla Alloy 3	F	130			Al-Si
Aural 2	F	140	310	8.6	Al-Si	LDHM -02	F	≥110	≥220	≥12	Al-Si
	T5	189– 230	303–339	8–9	Al-Si	ZL	F	123-141	276-298	14.7- 17.4	Al-Si
Aural 3	F	130– 160	250–310	4–8	Al-Si	THAS-	F	130~ 150	280~ 295	10~ 16%	Al-Si
	T5	190–24 0	300–340	4–6.5	Al-Si	JDA1	F	120-160	260~ 320	10~ 15	Al-Si
Aural 4	F	103	219	17	Al-Si	HT11	F	116	263	16.85	Al-Si

0											•
	T5	112	221	16	Al-Si	HT22	F	120	284	15.5	Al-Si
	Т6	170-	260–300	9–17	Al-Si	Tiantan	F	135~	270~	≥10	Al-Si
	10	235	200–300			S	Г	170	320	≥10	AI-SI
	F	125-	245–265	9–12	Al-Si	Magsi	F	160–220	310–340	12–18	Al-Mg
Aural 5	Г	145			Al-Si	mal 59	Г	100-220	310-340		Ai-wig
Aurai 3	T5	120-	190–260	6–12	A1 C:	Magsi	F	208	348	10	Al-Mg
	13	160	190–200	0-12	Al-Si	mal-plu	1	208	340		
Mercalloy A368	F	125-	260–275	10–12	Al-Si	s	T5	230–240	360–370	10	Al-Mg
	ľ	140	200–273			3	13	230-240	300–370	10	Ai-wig
	Т6	185-	280–295	14–16	Al-Si	Castad	F	123–135	245-265	11–15	Al-Mg
		200				uct-42	1				
	F	115	270	8.1	Al-Si	JDA2	F	$180\sim$	$360\sim$	8~12	Al-Mg
	1	113	270	0.1	711 51	05/12	•	220	420	0 12	711-1VIg
Mercalloy	T5	170-	295–310	5–9	Al-Si	560					
A367	10	205	2,0 010				F	150-156	262-274	17-	Al-Mg
	Т6	230–	295–340	8–10	Al-Si	560.1	1	150 150	202 274	23%	
	10	245	2,0 0.0	0 10		20011					
C611	F	117-132	228-268	10-	Al-Si						
COII	1	11/-132	220-200	14.1	711-51						

In recent years, notable progress has been made in China in the development of integrated die-cast aluminum alloys. LDHM 02, a non-heat-treatable aluminum alloy independently developed by LIZHONG GROUP, exhibits excellent die castability and mold filling capability, along with good high-temperature corrosion resistance, thermal stability, and electrical conductivity. Designed as a counterpart to Castasil 37, LDHM 02 adopts a low Mo modification technology, in which the Mo content is only one-fifth to one-seventh of that in comparable international modifiers. This approach effectively addresses the key issue of compositional segregation during large-scale integrated die casting. While enhancing performance, it also reduces manufacturing costs by 15 to 20 percent compared to similar foreign alloys, significantly improving the market competitiveness of domestically developed non-heat-treatable alloys^{[31],[39]}. The research team led by Liming Peng, developed a non-heat-treatable die-cast Al-Si alloy named JDA1. In addition to Sr modification for refining the eutectic Si phase, the alloy uniquely incorporates a combination of V and RE elements during processing. This composite addition of V and RE helps maintain the eutectic Si in a fine and dispersed form, thereby enhancing the alloy's ductility. The JDA1 alloy achieves a significant improvement in elongation without compromising tensile strength and has been included in the material database for General Motors' Cadillac $CT6^{[34]}$. In addition, Tsinghua University,

collaboration with FAW Group, has developed a high-toughness as-cast Al-Si die-cast alloy, as shown in Table 1. Unlike conventional die-cast alloys, the THAS 1 alloy contains trace additions of Zr and V, which serve to refine the grain structure and enhance solid solution strengthening and matrix strength. The alloy exhibits a yield strength of up to 130 MPa, an ultimate tensile strength in the range of 280 to 295 MPa, and an elongation of up to 16%^[33]. On this basis, the THAS 2 alloy was subsequently developed with the addition of 0.1-0.4 wt.% Mg and 0.1-0.4 wt.% Zn. By optimizing both the individual contents and the ratio of Mg to Zn, the alloy's strength was further enhanced[40]. The THAS 3 alloy, with additional Cr and Ti elements introduced to reduce the size of Fe-rich phases, exhibits excellent strength and ductility^[41]. China FAW introduced Mg and Cu into the alloy system and carefully controlled their relative ratio, promoting the formation of a finer AlSiCuMg phase. This design strategy enhances the alloy's strength without compromising its ductility^[37]. In contrast, Guangdong Hongtu developed the HT11 alloy by reducing the Mg content to limit the formation of Mg₂Si phases, thereby achieving a balance between strength and elongation that meets the mechanical performance requirements for automotive structural components^[35]. Xiaomi has simultaneously introduced Mg, Cu, and Zn into its alloy system, with the Zn content specifically controlled at 0.25%, to comprehensively enhance the alloy's strength and meet the fundamental performance requirements of electric drive housings^[36]. In addition, to address the issue of thermal stability, Chinalc has developed the ZL alloy, which exhibits excellent thermal resistance. After exposure at temperatures not exceeding 150 °C for 1000 hours, the mechanical properties show less than 10% degradation. The alloy demonstrates outstanding as-cast mechanical performance, with a yield strength exceeding 120 MPa and an elongation greater than 14%. These characteristics significantly improve the qualification rate of thin-walled die cast structural components and help reduce the production cost of automotive parts^[32].

2.2 Al - Mg alloy

2.2.1 Composition design

Compared with Al–Si alloys, Al–Mg die-cast alloys have attracted increasing attention as promising non-heat-treatable materials due to their high strength, excellent toughness, and superior corrosion resistance. However, their relatively high thermal expansion coefficient and solidification shrinkage limit their application range, which currently remains narrow and is

mainly focused on castings that require high corrosion resistance and superior surface quality. Commonly used non-heat-treatable Al–Mg alloys and their chemical compositions are listed in Table 3.

In Al-Mg alloys, Mg serves as the primary strengthening element, typically in the range of 3-12 wt.%. Mg mainly contributes to solid solution strengthening, making Al-Mg alloys well-suited for the development of non-heat-treatable aluminum alloys. To improve the castability of Al-Mg alloys, Si is usually added in the range of 0.8-1.3 wt.% to enhance melt fluidity and feeding ability during solidification. The microstructure of high-pressure die-cast Al-Mg alloys typically consists of an α-Al matrix with dissolved Mg atoms and a eutectic phase composed of α-Al + Mg₂Si. Using scanning transmission electron microscopy (STEM), Yuan^[42] captured bright-field and dark-field images of the typical morphology of Mg₂Si, as shown in Fig. 3. The Mg₂Si particles exhibit a short, rod-like morphology with elliptical ends. The lengths of these rod-shaped Mg₂Si particles range from 497.2 to 1064.7 nm, while their diameters vary between 118.1 and 258.8 nm.

Table3. Elemental content of Al-Mg series alloys

	Al-Mg										
Companies	alloy	Si	Fe	Cu	Mn	Mg	Zn	Ti	Sr	other	Ref
	system										
	Magsimal	1026	< 0.2	< 0.02	05.00	5060	0.07	< 0.2		Do	
	59	1.8–2.6	< 0.2	< 0.03	0.5–0.8	5.0–6.0	0.07	< 0.2		Be	
D1 : C11	Magsimal	2226	< 0.15	< 0.05	0.5-0.8	6.0–6.4	0.07	< 0.05		Mo,	[22]
Rheinfelden	-plus	2.2–2.6	< 0.15							Be, Zr	[22]
	Castaduct-	-0. 2		. 0. 2	-0.15	41.45	0.2	-O 2	-0.2	Б	
	42	< 0.2	1.5–1.7	< 0.2	< 0.15	4.1–4.5	0.3	< 0.2	< 0.2	Be	
Shanghai								0.15		Be,Ca,	
Jiao Tong	JDA2	2.0-3.6		< 0.04	0.6-0.9	6.0-8.0		0.15-		VRE,	[43]
University	University							0.20		Zr	
	5.00	0.25	0.2		1.10-	2.80-	0.05	0.15			
	560	0.25	0.2		1.40	3.60	0.05 0.15				
Alcoa					1.10-	2.85-					
	560.1	0.25	0.15		1.40 3.60		0.05	0.15			

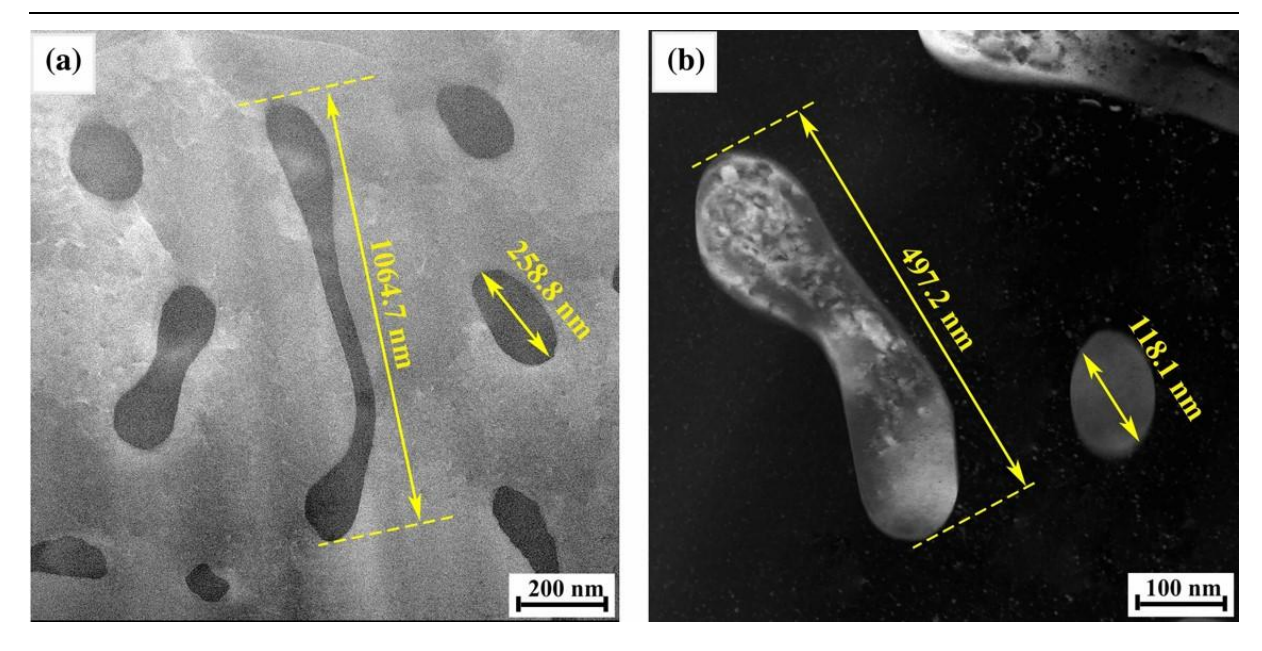


Fig. 3. Typical morphology of the Mg₂Si phase: (a) bright-field image; (b) annular dark-field image

The Zn plays a solid solution strengthening role in Al-Mg aluminum alloys, primarily through the formation of MgZn₂. In addition, Zn provides electrochemical protection, reducing the corrosion rate of Al-Mg alloys, particularly in humid or electrolyte-rich environments. Moreover, the presence of Zn improves the alloy's casting fluidity and formability, making Al-Mg alloys more suitable for the production of large and complex die-cast components, while also reducing casting defects such as cold shuts and porosity^[44]. In addition, properly controlling the Fe content can mitigate its detrimental effects on the mechanical properties of Al-Mg alloys. According to the findings of Zhu et al., when the Fe content is below 2.0%, its addition can enhance the ultimate tensile strength. However, as the Fe content increases further, the ultimate tensile strength decreases significantly. To achieve optimal overall mechanical performance, the Fe content should be maintained within the range of 2.0-2.5%^[45]. For non-heat-treatable alloys, controlling the content of porosity and inclusions is critical to ensuring desirable material properties. In Al-Mg alloys, Be is commonly used to improve the oxidation behavior of the melt. Due to the high reactivity of Mg with oxygen at elevated temperatures, excessive oxidation products can form and induce porosity defects. The addition of Be facilitates the formation of a dense and stable BeO film on the surface of the melt, which effectively isolates the melt from air exposure. This not only reduces oxidation losses and suppresses pore formation, but also lowers the oxygen content and defect rate in the alloy. In addition, Be also

serves as a modifying element that reduces the detrimental effects of Fe-rich phases and refines the size of eutectic silicon, thereby contributing to the improvement of both mechanical and fatigue properties of the alloy^[46].

2.2.2 Recent advances in domestic and international research The 560 series is a die-cast aluminum alloy developed by Alcoa in 2008. This alloy uses Mg and Mn as its primary alloying elements, both contributing to solid solution strengthening. Upon its development, the 560 alloy was promptly applied in the production of large-sized door components for the Nissan GT-R. However, due to its wide solidification temperature range, the alloy exhibits a strong tendency toward hot cracking during die casting. As a result, it is not the optimal choice for components with significant variations in wall thickness. Building upon the previously developed alloy, Alcoa introduced the A152 alloy with 3% magnesium and the A153 alloy with 4% magnesium to improve the hot cracking resistance. These modifications were aimed at enhancing the plasticity and cold formability of Al-Mg alloys^[47]. developed Magsimal59 Rheinfelden the (AlMg5Si2Mn), in which the addition of Si was employed to improve hot cracking resistance and enhance melt fluidity during the casting process. In the as-cast condition, the alloy exhibits a yield strength of 160 MPa, an ultimate tensile strength of 310 MPa, and an elongation of 12%. Another variant, Magsimal-Plus, achieves a high as-cast tensile strength of up to 340 MPa. In addition, this alloy exhibits excellent corrosion resistance, often eliminating the need for protective

coatings^[22]. Castaduct42 is another alloy developed by Rheinfelden. Compared to alloys such as C446F and Magsimal59, it features a lower Mn content and a relatively higher Fe content. This composition provides improved anti-soldering performance during die casting. Moreover, the alloy is well-suited for production using recycled aluminum, offering advantages in reducing carbon emissions.

The JDA2 alloy, developed by Peng's team in Shanghai Jiao Tong University, contains a high magnesium content, which tends to promote the formation of coarse eutectic Mg₂Si particles in the microstructure, thereby reducing the alloy's elongation. To address this issue, grain-refining elements such as Ti, Zr, and V were introduced, along with RE/Ca composite modifiers to refine the eutectic Mg₂Si phase. As a result, an optimized microstructure composed primarily of an α-Al matrix and fine eutectic Mg2Si was achieved. In the as-cast state, the alloy shows a yield strength of 210 MPa, tensile strength of 340 MPa, and elongation of 12.1%. Notably, after conventional die casting followed by natural ageing, its mechanical properties surpass those of Magsimal 59 alloy even after T6 heat treatment. This category of heat treatment-free die-cast aluminum alloys is particularly well-suited for manufacturing thin-walled automotive components^{[43],[48]}.

2.3 Other newly developed alloys

In addition to the aforementioned systems, many researchers have also focused on the development of other categories of non-heat-treatable alloys. Song et al. from the Institute of New Materials, Guangdong Academy of Sciences, independently developed a non-heat-treatable, high thermal conductivity die-cast aluminum alloy named GDAS. In this alloy, Zn is employed as the primary strengthening element. Due to its high solubility in aluminum, Zn mainly exists in the form of a solid solution, thereby enhancing the strength of the matrix. Without any heat treatment, the alloy achieves a tensile strength exceeding 320 MPa, a yield strength above 200 MPa, an elongation of over 8.0%, and a thermal conductivity greater than 160 W/(m·K). These properties make it highly suitable for manufacturing communication infrastructure components, such as base station housings and heat sinks^[49]. Li et al. from Shanghai Jiao Tong University developed non-heat-treatable high-strength and high-toughness die-cast Al-Ce-Mg-Si alloy. Unlike conventional Al-Si and Al-Mg die-cast aluminum alloys, this alloy incorporates 6-8 wt.% Ce, which promotes grain refinement by forming AlCeSi phases that serve as

nucleation sites for α-Al heterogeneous Furthermore, the presence of AlCeSi and Al₁₁Ce₃ phases as secondary particles contributes to second-phase strengthening. In the as-cast state, the alloy exhibits a yield strength exceeding 140 MPa, an ultimate tensile strength above 250 MPa, and an elongation greater than 10%, while maintaining excellent castability^[50]. Xiaomi has developed a die-cast Al-Cu-Mg-Zn aluminum alloy tailored for electric drive housings. The alloy exhibits a yield strength above 220 MPa and a tensile strength exceeding 330 MPa, meeting the structural performance requirements of the housing. However, its ductility remains relatively low^[51]. Similarly, NIO has developed a non-heat-treatable aluminum alloy for motor housing applications. Cu and Mg are added to the alloy, and the mass ratio of Cu to Mg is carefully controlled within a specific range to maximize strength enhancement compromising toughness. The without alloy demonstrates a tensile strength greater than 360 MPa, a yield strength above 230 MPa, and an elongation exceeding 3 %, making it suitable for use in motor housings^[52].

3 Effects of casting defects on microstructure and mechanical properties and process optimization

3.1 Types of casting defects

Fluctuations in die casting process parameters and improper operation inevitably lead to the formation of casting defects, which in turn manifest variations in defect types, sizes, and severity levels. A systematic analysis of different types of defects and their formation mechanisms can effectively guide process adjustments and thus improve product quality. Fiorese et al. reviewed the hierarchical classification methods for defects in aluminum castings^[53]. They categorized defects into: (1) defect morphology and location (internal, external, geometric); (2) metallurgical origins of defects (such as porosity, solidification shrinkage, etc.); and (3) specific defect types (noting that the same metallurgical phenomena may give rise to multiple defect types). This study builds upon the defect classifications summarized by Fiorese and Wang et al., refining them into four categories: internal defects, surface defects, geometric defects, and metallurgical defects. Fig. 4 illustrates the morphological characteristics of each defect type.

3.1.1 Internal defects

3.1.1.1 Shrinkage pores

During solidification, shrinkage pores are discontinuity defects caused by insufficient feeding of molten metal. These regions are typically the last to solidify, known as hot spots, and are usually located within the interior of the casting. In rare cases, they may appear near the surface, resulting in surface defects resembling shrinkage depressions. Based on their volume and distribution characteristics, shrinkage pores can be classified into macro-shrinkage pores and interdendritic shrinkage pores^[54]. Macro-shrinkage pores typically form in specific regions of the casting, such as thermal hot spots, and are characterized by rough surfaces and a spongy appearance. Interdendritic shrinkage pores mainly occur during the final stage of solidification. As dendrites solidify first in local regions, volume contraction arises. When liquid metal fails to sufficiently feed the interdendritic areas, shrinkage pores form. According to extensive work by our group, shrinkage pores in cast aluminum alloys range in size from a few micrometers to several millimeters and exhibit significant inhomogeneity in their distribution.

3.1.1.2 Gas pore, gas-shrinkage pore and blisters

Gas pores typically appear as spherical or elliptical cavities with relatively smooth surfaces and small sizes^[11]. A thin oxide film is often observed on the inner surface, resulting from reactions between air and molten

metal at high temperatures. Due to their distinct formation mechanism and geometry, gas pores are generally easy to identify in XCT or metallographic analyses and can be distinguished from shrinkage-related defects. Fig. 4 shows representative images of gas pore defects. Although small in size, such defects can still act as crack initiation sites under high stress or cyclic loading conditions^[55]. When gas pores become interconnected with shrinkage pores during solidification, they form gas-shrinkage pores. These pores exhibit typical hybrid characteristics, with an overall rounded morphology often accompanied by localized protrusions or elongated tails. Such features reflect the combined influence of internal gas pressure and solidification shrinkage during their formation, resulting in morphologies that are intermediate between isolated gas pores and shrinkage pores^[56]. When the internal pressure of gas pores near the surface is sufficiently high, it can induce plastic deformation of the casting surface at elevated temperatures, resulting in the formation of small surface bulges known as blisters^{[57],[58]}.

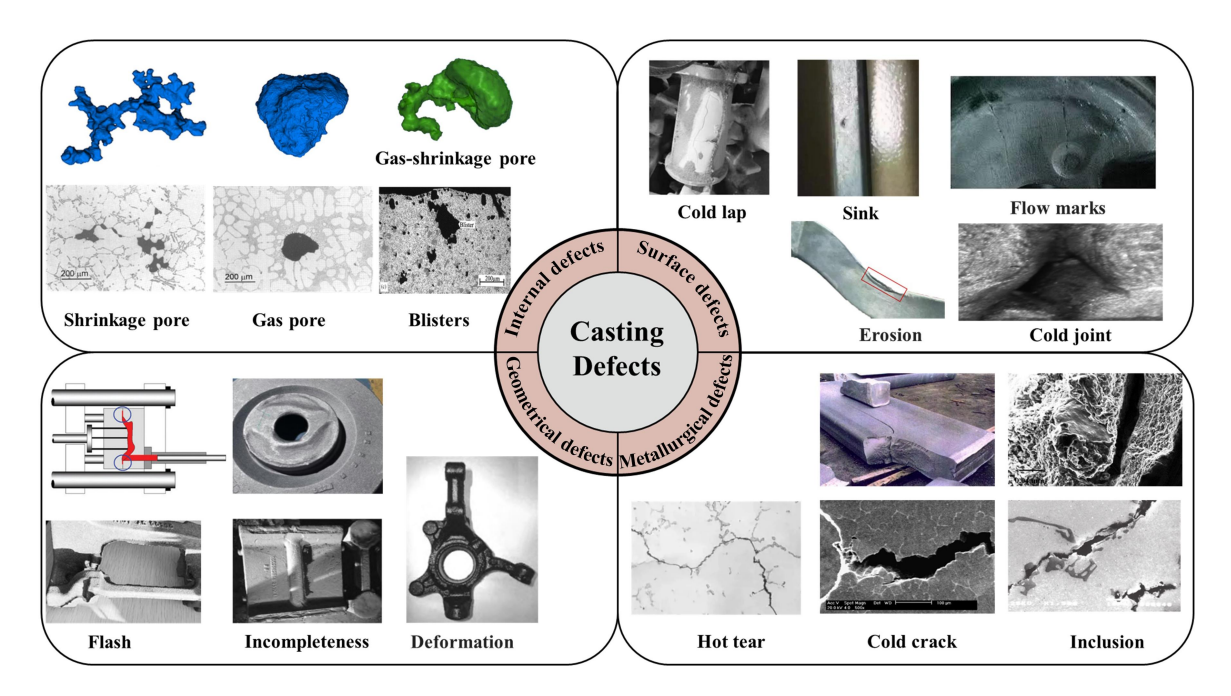


Fig.4 Multilevel classification of defects in aluminum alloy castings

3.1.2 Surface defects

Surface defects are typically attributed to abnormal surface conditions caused by interactions between the molten metal and the mold. Common types of such defects include sinks, flow marks, cold joints, surface sediment, erosion, indentations, cold laps, cold shots, and laminations. These defects are usually found in areas that

are heavily affected by the impingement of high-temperature molten metal or by severe thermal cycling.

3.1.2.1 Flow marks, cold joint, cold laps and cold shot Flow marks, cold joints, cold laps, and cold shots primarily originate from insufficient fluidity of the molten metal during mold filling, uneven temperature distribution, or inconsistent cooling rates. These conditions lead to poor metallurgical bonding or the entrapment of cold metal inclusions within the casting. Below is a brief overview of the formation mechanisms and characteristics of each defect type. Flow marks refer to surface stripes on the casting that follow the flow direction of the molten metal, accompanied by non-directional linear marks exhibiting a color difference from the metal matrix. The causes of flow marks include: (1) low mold temperature;(2) poor gating design, including unfavorable location of the internal gate;(3) low material temperature;(4) low filling velocity and short filling time;(5) inappropriate design of the pouring system; (6) defective ejector pins^[6]. Cold joints and cold laps both reflect inadequate fusion when multiple streams of molten metal meet. A cold joint is formed when two streams of molten metal fail to fuse completely upon meeting. Cold joints are especially prone to occur under conditions of low temperature, slow filling speed, and long metal flow paths, typically appearing as narrow and elongated defects. In contrast, a cold lap forms when a relatively cooler metal flow encounters another stream of molten metal at a higher temperature that remains fluid. This uneven thermal exchange affects the flow behavior of the molten metal, resulting in the formation of cold laps^[59]. In addition, cold shots differ from the previously described defects. When molten metal enters the mold in the form of droplets or splashes and rapidly solidifies upon contact with the mold wall, it may become entrapped within the casting under the impact of subsequently injected high-temperature metal, leading to the formation of cold shot defects^[53]. These defects often have a significant negative impact on the surface quality and overall structural integrity of the casting.

3.1.2.2 Surface sediment, erosion and indentations

Such defects fundamentally originate from the complex interactions between the mold and the molten metal in high-temperature and high-pressure environments. Surface sediments refer to a layer of material accumulated on the casting surface, which exhibits significant differences in chemical composition, thickness, distribution, and adhesion strength compared to the underlying substrate^[60]. In contrast, erosion is primarily caused by the repeated impingement of high-velocity molten metal on the mold surface, eventually leading to surface protrusions or pitting on the casting. This defect not only compromises the surface quality of the casting but may also reduce the service life of the mold. Such defects are typically attributed to

improper design of the location and geometry of the ingate, which results in abnormal flow direction and velocity of the molten metal. Additionally, indentations refer to marks caused by direct contact between the casting surface and the mold cavity surface, or to step-like depressions formed on the casting surface. These defects are typically associated with poor mold closure, surface damage to the mold, improper demolding, or non-standard operating procedures. They directly affect the surface appearance and dimensional accuracy of the casting.

3.1.2.3 Sinks

Sink marks are casting defects that occur as surface or near-surface depressions caused by solidification shrinkage of the metal during the casting process. They are commonly observed on the upper surfaces or in thick sections of castings, typically appearing as shallow or irregular indentations. Although the formation mechanisms of sink marks are similar to those of shrinkage porosity, their location near the surface classifies them as surface defects.

3.1.2.4 Laminations

Laminations, as a typical casting defect, refer to layered separations present within the casting or near its surface. They form when the molten metal comes into contact with the mold surface and rapidly solidifies, resulting in localized, distinctive layers inside the casting. Although both laminations and surface sediments manifest as thin layers, surface sediments are foreign materials adhering to the casting surface, whereas laminations are internal layered separations caused by incomplete fusion between two streams of molten metal or by entrapped oxides, gases, and other inclusions. Therefore, laminations are classified as forming defects. The main causes of laminations include insufficient fusion of the molten metal, improper gating system design, and poor mold venting.

3.1.3 Geometrical defects

Geometric defects refer to deviations of the actual casting shape from the design specifications caused by factors such as uneven material distribution, insufficient or excessive mold filling, and dimensional tolerances being exceeded. Common geometric defects include incomplete filling due to poor mold filling, flash resulting from mold misalignment, and deformation caused by uneven cooling or demolding stresses. These defects directly affect the dimensional accuracy and assembly performance of the casting.

3.1.3.1 Incompleteness and flash

During the mold filling process, insufficient molten

limited fluidity can easily metal or lead incompleteness, which is characterized by blurred contours and missing structural features. One of the fundamental causes of such defects is the high viscosity of the melt. In a highly viscous state, the melt exhibits increased flow resistance and has difficulty effectively filling thin-walled regions or complex features within the mold cavity. However, if an excessive amount of molten metal is present, it may infiltrate tiny gaps between the mold and the part, resulting in the formation of flash. When the clamping force provided by the die-casting machine is insufficient to counteract the internal pressure of the molten metal, the metal may escape along the mold's parting lines, thereby producing flash defects^[53].

3.1.3.2 Deformation

Deformation refers to the deviation of a casting from its intended geometric shape, primarily caused by thermal contraction during the cooling process. This defect tends to be more pronounced under high-temperature conditions or in castings with significant variations in wall thickness. Differences in solidification time and temperature across various regions of the casting generate internal stresses that cannot be fully relieved, resulting in the formation of residual stress and, consequently, deformation.

3.1.4 Metallurgical defects

3.1.4.1 Cold crack

Cold cracks are cracks that form in castings after solidification, as the temperature gradually decreases to lower levels, due to the effects of structural stress or residual stress. In high-pressure die casting (HPDC) processes, this defect typically occurs at lower temperatures, significantly below the alloy's solidification temperature range. Cold cracks are typically elongated and often manifest as transgranular fractures. As shown in Fig. 4, the presence of brittle intermetallic compounds within the alloy led to cold cracking, causing spontaneous fracture of a 500 kg aluminum alloy slab^[61].

3.1.4.2 Hot tear

Unlike cold cracks, hot tear form in the liquid phase within the mushy zone during the final stage of solidification. These cracks typically exhibit a dendritic morphology. Due to their formation at relatively high temperatures, the fracture surfaces are often accompanied by severe oxidation. This type of defect commonly occurs in alloys with a wide solidification range or in regions with thermal concentration, where the local stress, although significantly lower than the tensile strength of the alloy, is still sufficient to cause cracking

at the end of solidification^[62]. Fig. 4 shows the intergranular fracture characteristics of hot tear, with a tree-like propagation path.

3.1.4.3 Inclusion

Non-metallic or metallic compound phases that are present in the matrix and differ from it in both composition and structure are referred to as inclusions. According to their characteristics, inclusions can be classified into metallic and non-metallic types. The majority of inclusions are non-metallic, among which oxide inclusions are the most prevalent. Oxide inclusions are typically formed during the melting and pouring processes of the alloy. They result from complex chemical reactions between the charge materials, fluxes, modifiers, and atmospheric components such as oxygen and water vapour, and generally appear as thin films, flakes, or dispersed particles. Aluminum oxide, as the primary component of oxide inclusions, typically exists in the form of an oxide film. During pouring and mold filling, the folding and bending of the oxide film can lead to the formation of a double-layered structure known as a bifilm^{[63],[64]}. In the lower right corner of Fig. 4, a double-layered film structure is shown. A pore defect is located in the middle, and the bright white regions on both sides correspond to oxide films^[65].

3.2 Process optimization and defect control strategies

3.2.1 Integrated optimization strategy

As described above, casting defects are inevitably generated during the actual production of large integrated castings. Therefore, it is necessary to perform numerical simulations to predict micropore defects before practical design and development, allowing for the optimization of process parameters and the control of casting defects, ultimately improving the overall performance of the castings. At present, many researchers have adopted numerical simulation methods to comprehensively evaluate each process parameter. By employing optimization techniques, they aim to identify the optimal combination of parameters to enhance the performance of the cast components.

Dong et al. simulated the forming process of an integrated die-cast rear floor (IDCRF) using ProCAST^[66]. The simulation results revealed issues of delay and asymmetry during mold filling, which led to severe shrinkage pore defects. To reduce these defects, they employed the response surface methodology (RSM) to analyze the influence of key process parameters. The results indicated that pouring temperature had the greatest effect on the shrinkage pore volume, followed by mold temperature, fast shot velocity, and slow shot

velocity. By applying the optimal parameters determined through RSM, the simulation results, as shown in Fig.5(a), demonstrated a 59.1% reduction in the total shrinkage pores volume of the casting. This simulation-driven optimization strategy can significantly improve the quality and performance of large integrated aluminum alloy die castings. Kim et al. also addressed casting defect issues by proposing an optimization method that combines ProCAST simulation with a comprehensive quality index based on multi-attribute decision making^[67]. By converting multiple quality attributes into a single comprehensive quality index, they identified the optimal parameters for minimizing defects in AlSi9Cu1Mg alloy. The optimized parameters were a pouring temperature (PT) of 640 °C, a filling ratio (FR) of 40%, a piston velocity (PV) of 6.5 m/s, and a preheating mold temperature (PMT) of 150 °C. Among these, pouring temperature was again found to be the most critical process parameter affecting defect formation. Xu et al. adopted a similar method to comprehensively optimize the casting parameters, which ultimately minimized the porosity of the alloy^[68]. Our research group has conducted relevant work on investigating the influence of casting parameters on defect formation^[69]. Taking aluminum wheels as the research object, we used the ProCAST system to study the effects of process parameters, including pouring temperature, mold temperature, filling temperature, and holding pressure, on shrinkage pores. The results indicated that, within a certain range, increases in pouring temperature and mold preheating temperature improved the mold filling capability of the molten metal, thereby reducing shrinkage pores. However, when either the pouring temperature or the mold preheating temperature became excessively high, shrinkage pores began to increase. In recent years, with the widespread application of machine learning and artificial intelligence algorithms, some researchers have begun to use advanced computational methods to optimize process parameters in die casting. Shahane et al. proposed and validated a method that integrates a non-dominated sorting genetic algorithm (NSGA II), deep neural networks, and finite volume simulation to optimize the solidification process in die casting^[70]. In this method, product quality was evaluated as a function of the initial molten metal temperature and the boundary temperature. By adjusting the initial temperature and the mold temperature, optimal control of product quality was achieved. This research direction is expected to become a major focus in the future development of numerical simulation in the casting industry.

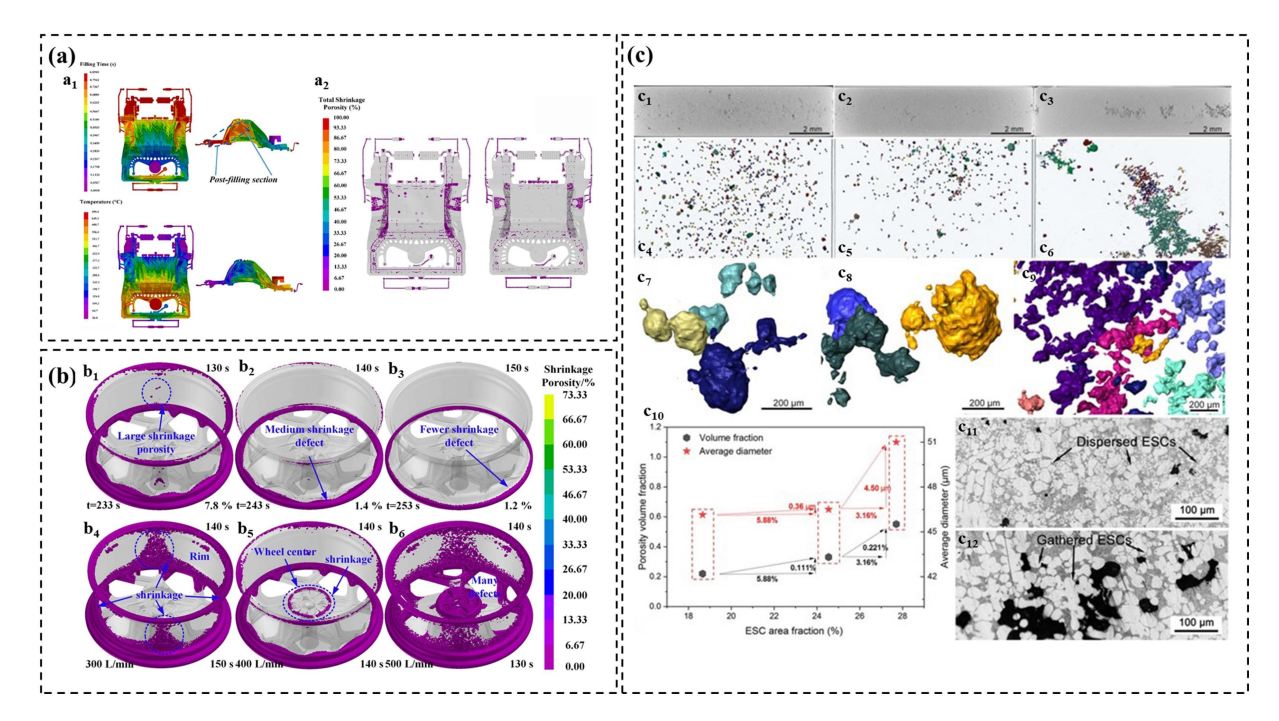


Fig. 5. (a) Forming simulation of the integrated die-cast rear floor (IDCRF); (b) sequential solidification simulation of a wheel under low-pressure casting; (c) micropore distribution under different injection speeds



3.2.2 Single-parameter optimization strategy

For key process parameters such as pressure, vacuum level, die casting speed, pouring temperature, and mold temperature, extensive research has already been conducted by many researchers. Die casting pressure plays a vital role in obtaining a compact microstructure and minimizing defects.

Yang et al. employed a vacuum-assisted high-pressure die casting process to fabricate large integrated castings under three different dynamic casting pressures^[71]. XCT was used to quantify the pore defects at each pressure level. At 390 bar, the porosity of the sample was reduced by 88.46% and 62.5% compared to those cast at 266 bar and 300 bar, respectively. Meanwhile, the yield strength of the casting produced at 390 bar increased by 5.59% and 12.32% compared to those cast at 266 bar and 300 bar, respectively. In addition, according to the actual die casting process, the pressure ratio can be categorized into the first-stage injection pressure ratio (IPR) and the second-stage boosting pressure ratio (BPR). In practical production, the selection of IPR should take into account various factors, including the geometry, size, complexity, and wall thickness of the casting, as well as the alloy and temperature. The literature summarized the criteria for selecting these pressure parameters^[6].

Vacuum level is primarily applied in high-pressure die casting, and previous studies have indicated that the number and size of defects in large castings produced under ultra-high vacuum conditions can be significantly reduced. For example, Cao et al. conducted simulations using Magma to compare vacuum die casting with conventional high-pressure die casting. The results showed that during vacuum die casting, the local certain regions of pressure in the casting was lower than that significantly in conventional high-pressure die casting^[72]. As the absolute pressure in the mold cavity decreases, both the number and size of porosity defects in the casting are significantly reduced. Szalva et al. also employed a vacuum-assisted high-pressure die casting process with three absolute pressures set at 170, 190, and 70 mbar. They found that reducing the mold cavity pressure significantly decreased both the porosity rate and pore size in the castings. When the pressure was lowered to 70 mbar, the porosity rate was reduced by as much as 57%[73]. Building on the above work, Yang et al. developed a three-stage ultra-high vacuum assisted process, successfully achieving a vacuum level below 50 mbar^[74]. The minimum and average vacuum levels within the entire

mold cavity reached 10 mbar and 23.4 mbar, respectively, surpassing the results reported in the published study^[6]. The microstructure obtained by ultra-high vacuum high-pressure die casting is denser and finer, with fewer porosity defects.

In addition, the injection speed is also a critical factor affecting casting quality. It is generally divided into slow injection speed and fast injection speed. Dou et al. investigated the effect of different slow injection speeds of the plunger on the mechanical properties of A356 alloy. The results showed that increasing the slow injection speed led to a more uniform distribution of surface oxides and a gradual reduction in porosity^[75]. Kim et al. investigated the influence of injection speed on segregation behavior, and the experimental results indicated that injection speed had the most significant effect on liquid-phase segregation. Therefore, this parameter must be strictly controlled^[76]. Jiao et al. investigated the influence of injection speed on alloy defects under high-pressure die casting using XCT. For rod-shaped samples, a moderate reduction in fast injection speed was found to decrease porosity, and the radial distribution of pores nearly disappeared. However, the proportion of irregular shrinkage pores increased. In contrast, for plate-shaped samples, reducing the fast injection speed led to an increase in porosity and promoted the formation of large shrinkage pores. This phenomenon is closely related to the accumulation of externally solidified crystals (ESCs). The distribution of pores under different injection speeds is shown in Fig. 5(c).

Even with well-controlled vacuum level and injection speed, neglecting temperature parameters can still lead to the formation of large-sized pores in castings. If the pouring temperature is too high, coarse grains may form in the casting, increasing the risk of cracking. Conversely, if the pouring temperature is too low, defects such as cold segregation, surface marks, and incomplete filling are likely to occur. In addition, previous studies have shown that increasing the mold temperature is beneficial for improving the castability of large castings[60]. Therefore, when the mold temperature is excessively appropriate cooling measures should implemented. Dong et al. conducted numerical simulations of the low-pressure casting process for A356 alloy wheels to investigate the effects of cooling parameters and holding time on the forming quality. The results showed that at a cooling flow rate of 400 L/h and a holding time of 140 s, sequential solidification occurred in the rim region, effectively preventing defect formation, as shown in Fig. 5(b)[77]. Experimental results



further confirmed that a refined secondary dendrite arm spacing (SDAS) and uniformly distributed eutectic silicon were the fundamental reasons for the improved mechanical properties.

3.3 The influence of casting defects on mechanical properties

3.3.1 Porosity

Lee systematically investigated the correlation between porosity and mechanical properties in 2007^[78]. He found that porosity exhibited a linear relationship with tensile strength and an inverse parabolic relationship with elongation, and further demonstrated that fracture-based constitutive predictions provided a more accurate estimation of the overall tensile performance of A356 alloy than those based solely on volumetric porosity. Lordan proposed a novel estimation approach, referred to as Z-Project, which enables highly accurate prediction of the area fraction of voids during tensile fracture, significantly outperforming previous methods^[79]. As illustrated in Fig. 6(a), the Z-Project method achieves improved prediction accuracy for both tensile fracture strain and fracture strength by integrating the estimated void area fraction with an existing plastic instability evolution model. Similarly, Kong et al. conducted a study on specimens from different regions of low-pressure cast wheels and found that elongation decreased with increasing porosity and SDAS^[80]. Based on experimental data and numerical simulations, they developed a constitutive model describing the effect of porosity on flow stress, as well as a damage model characterizing the relationship between fracture strain, porosity, and stress triaxiality. In addition, Zhang et al. found that the local porosity in the fracture region of die-cast alloy specimens exhibited a stronger correlation with elongation. However, since measuring porosity directly in the fracture region is challenging, the authors proposed estimating the variation in ductility using the maximum local porosity within the gauge section obtained before tensile testing. As shown in Fig. 6(b), a functional relationship between the maximum local porosity and elongation was established^[81]. Zhang et al. also investigated the quantitative relationship between porosity and Young's modulus^[82]. In summary, porosity is closely related to mechanical properties, and the development of constitutive models based on porosity can lead to more accurate predictions of the mechanical performance of cast components.

3.3.2 Maximum micropore size

Micropore size has a significant influence on the mechanical properties and fatigue life of materials,

among which the maximum micropore size plays a dominant role as a critical factor in crack initiation and propagation. At present, numerous studies have investigated the quantitative relationships between maximum micropore size, elongation, and fatigue life. Teng et al. conducted tensile tests on 30 cylindrical specimens to establish the relationship between elongation and micropore size^[83]. The study revealed that elongation exhibited an approximately linear correlation with the maximum projected micropore area. Liu et al. similarly found that elongation is closely related to the volume fraction of the largest micropore within the gauge section, and that fracture tends to initiate preferentially at the location of the largest micropore in the specimen^[84]. Therefore, by using XCT scanning to characterize micropore defects in castings determining the volume fraction of the largest micropore in the specimen, elongation can be estimated. Zhang et al. found that in T6 heat-treated alloys, the maximum micropore size is negatively correlated with elongation. Furthermore, based on experimental results, the level of microporosity is a key factor influencing the variability of mechanical properties. When the micropore size is less than 0.3 mm, its adverse effect on the mechanical performance of the alloy can be considered negligible^[85]. Additionally, Tebaldini et al. defined the maximum micropore size in the spoke region as the Maximum Feret Diameter and used calculation and fitting methods to predict the fatigue limit of A356 wheels^[86]. Ren et al. further incorporated micropore size, location, shape, and other parameters to refine the fatigue model^[87]. Streck et al. proposed a novel clustering method based on 3D volumetric data^[88]. In this method, two micropores are considered to interact and are treated as a single larger "equivalent defect" if the center-to-center distance between them is smaller than the diameter of the smaller micropore. This approach enhances the capability of defect-based fracture mechanics analysis and enables the identification of critical micropores that interact with stress concentration zones, thereby providing more accurate failure predictions for die-cast aluminum alloys. In addition to micropore size, similar quantitative have been observed between relationships microstructure and mechanical properties of Al-Si alloys. Yan et al. systematically investigated the effects of SDAS, grain size, and eutectic silicon on the mechanical behavior of various cast Al7Si1.5Cu0.4Mg alloys. The results showed that both grain size and SDAS follow the classical Hall-Petch relationship with respect to yield strength. Furthermore, a predictive model for ultimate

tensile strength was established, along with a novel Tensile–Fatigue Bridge Model, which serves to bridge tensile behavior and fatigue performance, ultimately enabling the evaluation of non-uniform mechanical properties^[89].

3.3.3 Micropore morphology

Micropore morphology is primarily distinguished based on sphericity. Typically, micropores with a sphericity less than 0.4 are classified as shrinkage pores, while those with a sphericity greater than 0.4 are considered gas pores^[90]. The shape of micropores influences stress concentration, which can ultimately lead to fracture^[91]. Numerous researchers have conducted studies on this subject.

Nicoletto et al. investigated the influence of casting micropore morphology on stress concentration and found that shrinkage pores exhibit higher stress concentration factors than gas pores. Moreover, the average stress concentration induced by actual micropores was found to be greater than that of ideal spherical micropores^[92].

Le et al. performed finite element simulations on spherical and oblate-spheroidal micropores and observed that, under the same equivalent diameter, the normalized Dang Van equivalent stress was higher for oblate-spheroidal micropores^[93]. In summary, there is a consensus in the existing literature that the morphology of micropores has a significant influence on the stress state at their surfaces. Chaijaruwanich et al. quantitatively investigated the behavior of micropores homogenization process of cast aluminum alloys. With increasing homogenization time, the micropore shape factor decreased significantly, and coarsening occurred in local micropore regions. This phenomenon was primarily attributed to Ostwald ripening within the micropores^[94]. In addition, some researchers have developed cellular automaton models to simulate the evolution of the three-dimensional morphology of micropores during alloy solidification, and have identified the key influencing factors^{[95],[96]}.

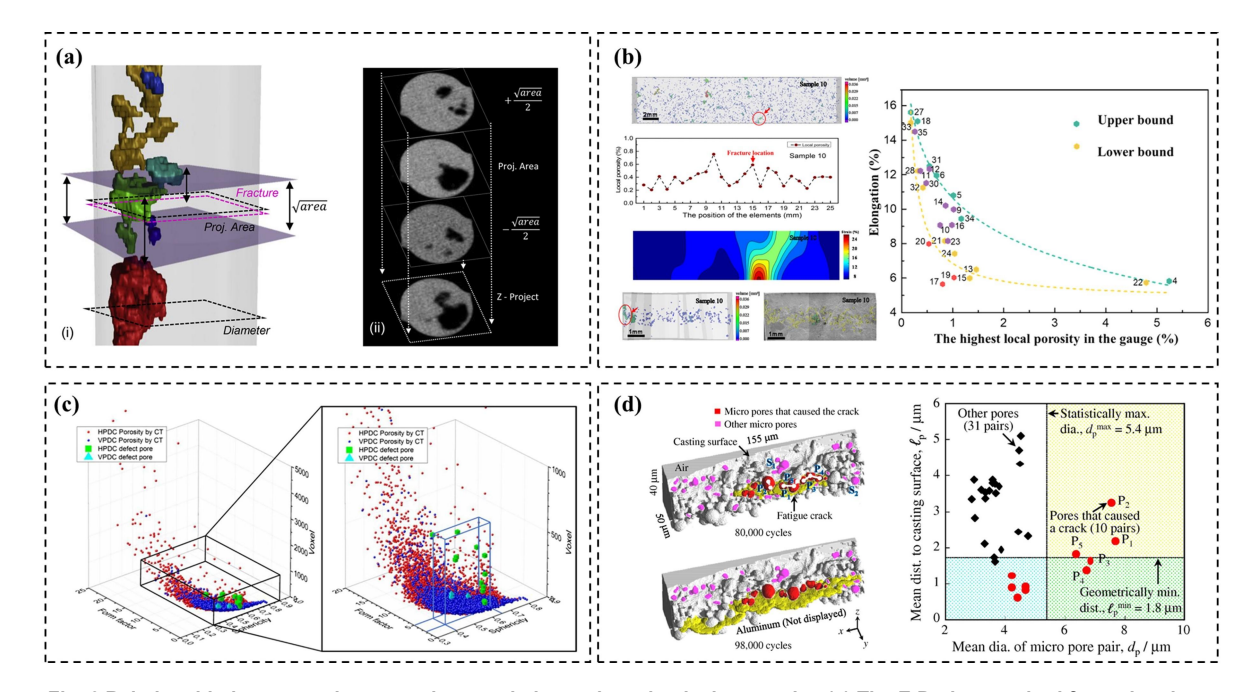


Fig. 6 Relationship between micropore characteristics and mechanical properties:(a) The Z-Project method for estimating projected micropore area; (b) functional relationship between maximum local porosity and elongation;(c) detected porosity visualized as a function of sphericity, shape factor, and defect volume using CT;(d) schematic illustration of fatigue crack initiation behavior near the surface and the spatial relationship between paired micropores and the casting surface.

3.3.4 Micropore distribution and location

Apart from porosity, micropore size and morphology, the location of micropores is a crucial parameter. Yi and Le et al. suggested that large micropores or oxide films located on or near the specimen surface serve as favorable sites for crack initiation^[97]. However, in the

absence of such surface or near-surface defects, the fatigue performance of the alloy is primarily governed by the eutectic silicon particles within the material. Li et al. [14] pointed out that the initiation and propagation of fatigue cracks are influenced by the maximum local stress concentrations caused by micropores near free

surfaces and crack tips[98]. Serrano-Muñoz et al. [15] also investigated the effect of internal defects on the fatigue life of aluminum alloy castings. They found that both the crack initiation and propagation rates at internal defect sites were significantly lower than those at surface defects. This observation indicates that internal defects have a less pronounced impact on fatigue life compared to surface defects^[99]. Szalva conducted an innovative analysis of all micropore characteristics and visualized them in a three-dimensional coordinate system defined by sphericity, shape factor, and defect volume, as shown in Fig. 6(c). The results revealed a distinct trend among these micropore features. Despite a wide numerical range of boundary conditions, the material heterogeneities leading to final fracture were found to cluster within a significantly narrower region, highlighted by the blue wireframe column in the figure. Ultimately, it was concluded that the location and size of casting defects are the primary factors determining the fatigue life of the specimens^[100]. Micropores located near the surface can significantly influence fatigue crack initiation. Toda employed high-resolution XCT combined with statistical methods to investigate the geometric parameters that govern the relationship between micropores and fatigue crack initiation. The results indicated that the average diameter of micropore pairs and their average distance from the casting surface are the primary factors controlling crack initiation^[101]. Fig. 6(d) illustrates the crack initiation behavior originating near the specimen surface, along with a schematic representation of the relationship between the average diameter of micropore pairs and their average distance to the surface.

3.3.5 New perspectives on micropore defect and mechanical properties

3.3.5.1 X-ray computed tomography

X-Ray Computed tomography (XCT), as an advanced non-destructive testing technique, enables high-resolution three-dimensional visualization and quantitative characterization of internal micropore defects in castings. Currently, XCT-based reconstruction of three-dimensional mesh models incorporating real defects, followed by their implementation in finite element analysis, has become one of the key approaches for investigating damage mechanisms under complex stress states. Yang et al. employed XCT to obtain three-dimensional structures containing realistic defect distributions, which were subsequently used as input for finite element modeling^[102]. The damage initiation mechanisms of cast aluminum alloys under complex stress states were investigated from the microscale to the macroscale. The

study revealed that crack propagation primarily occurs through two microporosity-driven coalescence mechanisms: (1) micropore aggregation induces internal necking and stress concentration, thereby initiating cracks; and (2) cracks propagate along specific directions and further coalesce, ultimately leading to fracture. Moreover, this approach has been widely adopted in numerous studies to investigate damage mechanisms^{[91],[103]}. Our research team has conducted foundational work in this area. By employing XCT, finite element analysis, and digital volume correlation (DVC), systematically investigated the effects of micropore size, morphology, and spatial distribution at different positions within the wheel hub on its mechanical properties. The results demonstrated that the ratio of micropore projected area to the shortest distance from the free surface (PA/SD) exhibited the strongest correlation with the stress concentration factor (K) around the micropores, with a correlation coefficient as high as 0.90, and showed a clear linear relationship. Therefore, effectively eliminating large micropores near the edges can significantly enhance the mechanical performance of automotive wheel hubs^[104]. Wang and Li developed a multiscale fatigue life prediction method for automotive wheel hubs that simultaneously considers hydrogen porosity, shrinkage pores, and SDAS[105]. A three-dimensional cellular automaton (CA) model was employed to simulate dendrite growth and hydrogen pore concurrently. Additionally, a database correlating pore equivalent diameters with casting conditions was established. This database was mapped onto the structural mesh using an efficient grid mapping algorithm to facilitate both static and dynamic finite element simulations. Ultimately, a multiscale fatigue life prediction model for the wheel hub was constructed, incorporating the corresponding S-N curves at each mesh node, enabling accurate prediction of the lateral fatigue life of automotive wheel hubs. Additionally, team member Li employed laboratory XCT and the Shanghai Synchrotron Radiation Facility to investigate the influence of internal micropore defects on the mechanical properties of alloys during solidification, tensile deformation, and under various heat treatment conditions[106]-[108].

3.3.5.2 Machine learning

On the other hand, the use of machine learning methods to predict material performance based on defect parameters and processing conditions as inputs has become a current research hotspot^[109]. Kazup et al. proposed a bivariate analysis combined with machine learning regression modeling approach to systematically

investigate the relationship between pore characteristic parameters and mechanical properties of A356 castings. As shown in Fig. 7(a), Spearman's correlation coefficients were used to explore the linear relationships between any two pore characteristic parameters. Fig. 7(b) presents the ranking of mean importance scores calculated based on the optimal model. The results ultimately revealed that total deformation is mainly influenced by the pore location on the fracture cross-section and the porosity on the fracture surface^[110]. Zhai et al. established the Gurson-Tvergaard-Needleman (GTN) damage model to predict the mechanical properties by introducing a novel identification framework that integrates machine learning methods optimization algorithms^[111]. This approach effectively overcomes the high cost and low efficiency associated with traditional parameter identification methods. Chen et al. proposed a method that applies machine learning to the prediction and understanding of surface-related defects in castings. By correlating production data with defect data, six models were trained, and the results were interpreted and analyzed using the SHAP framework^[112]. Yang et al. employed a high-vacuum die casting process with a clamping force of 1800 tons to fabricate 3500 mm-long S-shaped structural castings^[113]. They investigated the effects of alloy composition, flow length, and filling time on mechanical properties and defect formation. The study

revealed that flow length significantly influences microstructural uniformity and porosity distribution. Through random forest regression analysis, alloy composition was identified as the dominant factor affecting strength, while flow length was found to play a decisive role in determining ductility. Hou et al. generated a comprehensive porosity dataset comprising 472 samples using three-dimensional cellular automaton simulations, and compiled an additional dataset of SDAS containing 310 samples from published literature. Seven artificial intelligence algorithms were systematically evaluated, among which extreme gradient boosting (XGBoost) was identified as the most robust model for microstructure prediction. SHAP analysis was further employed to reveal the influence of alloying elements processing parameters on microstructural features[114]. In addition, Yang et al. developed a methodology that integrates casting techniques with data-driven approaches to establish a framework^[115]. process-defect-property correlation Temperature data from different locations were used as input for a convolutional neural network (CNN), with mechanical properties as the output. This model enabled the prediction of mechanical performance at previously untested locations. Therefore, machine learning methods offer a fast and effective means of identifying the micropores correlation between and mechanical properties.

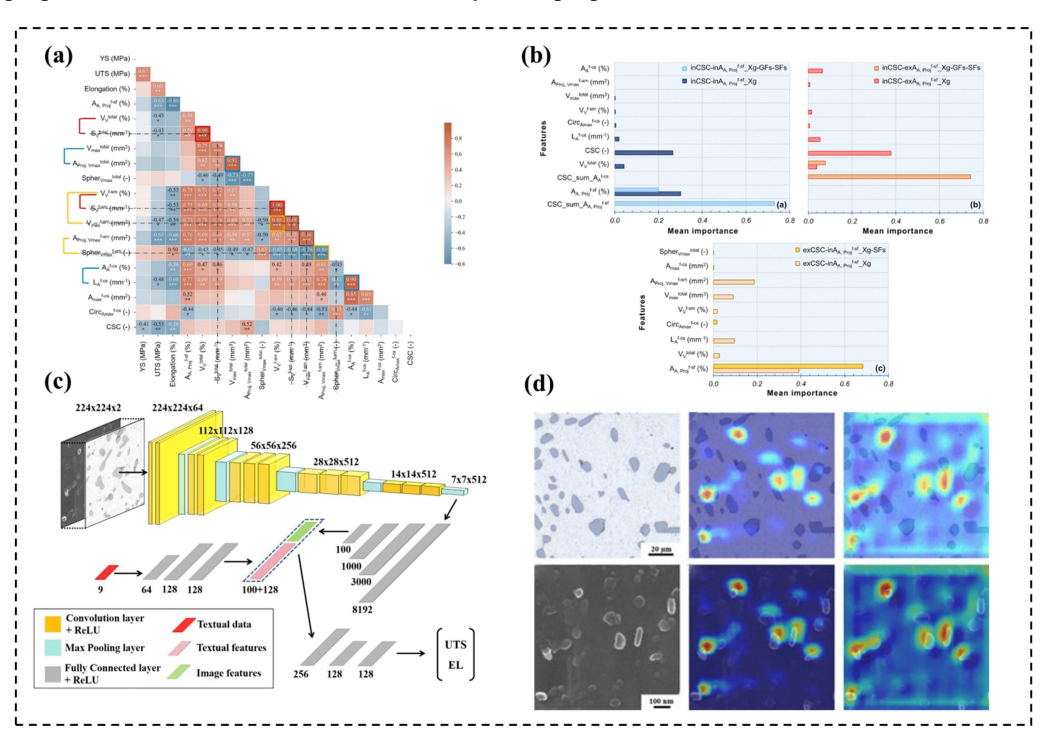


Fig.7 (a) Linear relationships between any two porosity feature parameters; (b) ranking of average importance scores for porosity feature parameters; (c) framework of the interpretable deep learning model; (d) visualization analysis of the model.



3.3.5.3 Image processing techniques

Accurate quantitative characterization of the material's microstructure is essential for exploring the relationship between microstructure and mechanical properties. Currently, image recognition combined with data-driven approaches provides a reliable solution for predicting the performance of complex cast components. Li et al. proposed a novel method for microstructural feature extraction based on the large visual model MatSAM^[116]. This approach demonstrates strong generalization capabilities for various microstructural features, including secondary phases, defects, and grain boundaries. Building upon this model, further predictions of alloy mechanical properties can be achieved. Wu proposed a Haar Dual-Domain Network (HDD-Net) for ring artifact correction^[117]. This method effectively separates and removes ring artifacts while preserving low-contrast microstructural features, offering a valuable technical reference for processing a series of noise-contaminated images. Ma et al. developed an interpretable deep learning model by using optical microscopy and SEM images as inputs[118]. As shown in Fig. 7(c), a multimodal and multiscale dataset was constructed to predict the tensile properties of aluminum alloys. Visualization techniques were also introduced to further reveal the internal mechanisms of the deep learning model, with Fig. 7(d) presenting the results of the model's visualization analysis. Guru et al. also developed a generalized machine learning workflow for performance prediction based on microstructure and texture descriptors[119]. Additionally, Ren et al. developed a generalized deep learning framework capable of handling multimodal databases that include compositional information and multi-source microstructural images. This framework enables accurate prediction of ultimate tensile strength and elongation across a wide range of stress-strain values[120]. In summary, methods based on image processing techniques and multimodal machine learning are gradually overcoming the limitations of traditional modeling, providing efficient and scalable solutions for performance prediction of complex castings. These research achievements lay a solid foundation for developing more universal composition-microstructure-property relationship models.

4 Application prospects of integrated die casting technology

4.1 Technical advantages

Since Tesla introduced integrated die casting technology in 2019, its development has driven a profound transformation in the automotive manufacturing sector by significantly enhancing component performance, production efficiency, and cost-effectiveness. This technology demonstrates four key advantages: (1) In terms of production cost, it eliminates the need for numerous welding auxiliary equipment, robotic systems, and other production facilities, thereby optimizing space utilization and reducing manufacturing expenses. (2) Regarding lightweight design, the integrated fabrication reduces vehicle body weight, which in turn decreases battery requirements. (3) In production efficiency, the traditional vehicle body manufacturing process involves over 500 individual parts that require separate fabrication and extensive stamping and welding operations. However, integrated die casting technology simplifies the process, reduces workload, and improves production accuracy^{[6],[121]}. (4) Concerning safety performance, this technology addresses the strength issues of aluminum alloy weld joints, enhancing structural integrity and body strength, thereby improving vehicle driving stability.

4.2 Typical applications

With the gradual advancement of integrated technology, not only can lightweight design be achieved, but the technical advantages of integrating multiple components can also be maximized. Currently, integrated die casting technology is primarily applied to the rear floor, front floor, and front engine compartment in complete vehicle manufacturing. Leading new energy manufacturers have swiftly adopted this technology, with Tesla, XPeng, AITO, and Xiaomi at the forefront in implementing large-scale integrated die-cast body structural components in mass-produced vehicles^{[6],[22]}. Fig. 8 illustrates the clamping force configuration of large die casting machines. Tesla's Cybertruck series continues the technical approach of the Model Y, employing a die casting machine with a clamping force of 90,000 kN to manufacture the front engine compartment and rear floor. The AITO M9 model produces an integrated rear floor and front compartment structure using the same 90,000 kN clamping force die casting machine. This structure integrates components, reduces welding points by 1,440, and increases torsional stiffness by 23%. XPeng G6's extra-large rear floor structure integrates components and utilizes die casting equipment with a maximum clamping force of 120,000 kN, representing the current highest clamping force. Additionally, a 160,000 kN die casting machine is under installation, which will be used for battery pack component production in the future.

4.3 Challenges and development trends

Although integrated die casting technology offers numerous advantages in automotive manufacturing, a series of pressing challenges remain to be addressed in its large-scale application. To begin with, the maturity of integrated die casting equipment remains relatively low. As the level of integration in die-cast structural components continues to increase, higher demands are placed on the tonnage and functionality of die casting machines, particularly in terms of clamping force and injection speed. However, the development and application of ultra-large die casting equipment are still in their early stages, and achieving reliable, industrial-scale deployment will require considerable time. For instance, these structures exhibit poor reparability. Once the vehicle body is damaged, the current technology does not allow for simple repairs, and complete replacement is often the only option. Secondly, the product qualification rate remains low. The increased size and structural complexity of die-cast components significantly raise the risks associated with mold filling and defect control, thereby substantially increasing the difficulty of the die casting process. At present, the qualification rate for integrated structural components generally ranges between 40% and 60%, indicating a relatively low overall yield. In addition, the coordination of auxiliary die casting equipment is relatively poor. Although integrated die casting simplifies the production process by eliminating numerous process steps and supporting equipment, it significantly increases reliance on auxiliary systems such as temperature control, spraying, and mold cooling. This places higher demands on system integration and automated control within the entire die casting unit.

To address these challenges, future development trends may include the following directions: The first

major trend is the development and intelligent upgrade of large-scale die-casting equipment, as the machinery directly affects the quality and dimensional accuracy of cast parts. Currently, only a few manufacturers worldwide can produce ultra-large die-casting machines with clamping forces exceeding 60,000 kN, such as Swiss Bühler, Haitian Metal, Yizumi, and Lijin Technology along with its subsidiary brand IDRA. The production of extra-large structural components not only requires powerful equipment but also calls for systemic breakthroughs in theoretical modeling, mold design, temperature-control and forming expertise. technologies, advancements in simulation modeling and parallel computing have become essential tools for addressing the challenges posed by increasingly complex die casting processes. As the structural complexity of die-cast components continues to grow, higher precision is required predicting mold filling in solidification processes, and thermal field distribution. Process simulations involving multi-scale and multi-physics coupling are progressively relying on high-performance computing platforms. Moreover, intelligent algorithms such as machine learning are being introduced to optimize process parameters, thereby enhancing both the efficiency and accuracy of simulations. Thirdly, guided by the integrated computational materials engineering (ICME) framework, the establishment of end-to-end models linking composition, casting processes, microstructural evolution, and service performance is driving the rapid development of aluminum alloys tailored for integrated die casting. By constructing multiscale coupled models and incorporating artificial intelligence-based optimization algorithms, it becomes possible to design high-strength, high-toughness, non-heat-treated alloys that meet the specific requirements of die casting applications.

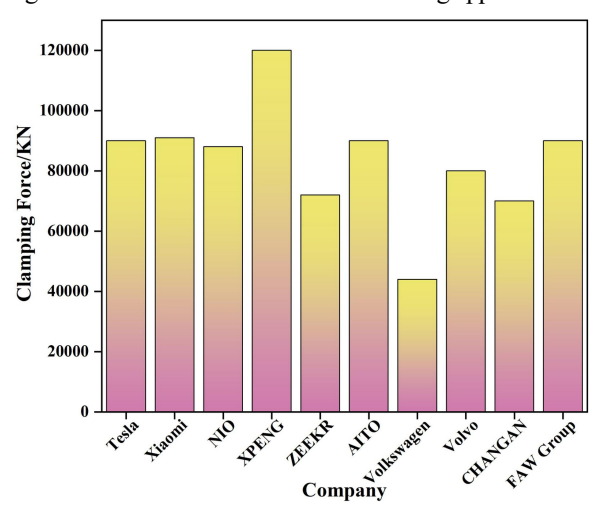


Fig. 8 Integrated die casting machine configurations of various automakers

5 Conclusion

This paper provides a focused review of recent advances in integrated die-cast aluminum alloys, systematically analyzing the mechanisms by which casting defects and process parameters influence mechanical properties. It also explores the potential applications of this technology in industrial settings. Therefore, the following conclusions can be drawn.

- (1) Currently, lightweight alloys used for integrated die casting in non-heat-treatable manufacturing are predominantly based on Al-Si and Al-Mg systems. Strengthening and toughening of these alloys are mainly achieved through microalloying design combined with solid solution strengthening and grain refinement. The development of a new generation of non-heat-treatable alloys that balance strength, corrosion resistance, and recyclability for large-scale, complex die-cast components by integrating data-driven approaches and intelligent algorithms is expected to become a key research focus in the field of aluminum alloy materials.
- (2) Compared to traditional die casting technology, integrated die casting imposes higher technical requirements on materials, molds, processes, and equipment. In particular, regarding production factors, the use of simulation to design and optimize multiple parameters such as injection pressure, filling velocity, filling time, holding pressure time, mold temperature, and cooling system design has become an essential approach for advancing integrated die casting processes.
- (3) This study systematically summarizes the intrinsic relationships between casting defects and the mechanical properties of materials, with a focus on the influence mechanisms of porosity, maximum micropore size, micropore morphology, spatial distribution, and location. The research demonstrates that micropore characteristic parameters play a dominant role in damage initiation and crack propagation, directly affecting the service performance of materials. A thorough understanding and modeling of the damage mechanisms related to pore failure are of critical importance for achieving defect control and performance prediction. The integration of high-resolution XCT with machine learning, advanced image processing models, and artificial intelligence algorithms to develop data-driven models capable of predicting the performance of large, complex die-cast components will be a key focus of future research.
- (4) The rapid growth of the new energy vehicle industry has provided a strong driving force for the development of integrated die-cast aluminum alloy

materials and the manufacturing of ultra-large integrated die casting equipment in China. The development of large, complex thin-walled structural components requires a high degree of collaboration across multiple fields, including materials design, forming process development, die casting machinery, ultra-large molds, numerical simulation, and auxiliary software. Only by establishing a complete industrial chain can the high-quality development and mass production of giant castings be achieved.

References

- [1] Merklein, M, Geiger, M. New Materials and Production Technologies for Innovative Lightweight Constructions. Journal of Materials Processing Technology 2002, 125 -126, 532 - 536.
- [2] Shen, J, Zhang, Q, Tian, S. Impact of the Vehicle Lightweighting and Electrification on the Trend of Carbon Emissions from Automotive Materials. Journal of Cleaner Production 2025, 513, 145677.
- [3] Villanueva, E, Vicario, I, Crespo, I, Guraya, T,et al. Development of a New Ductile Heat-Treated Multi-Component Aluminium by HPDC with High-Performance Properties for Temperature Applications. Journal of Alloys and Compounds 2025, 1020, 179146.
- [4] Merchán, M, Egizabal, P, García de Cortázar, M, Irazustabarrena, A,et al. Development of an Innovative Low Pressure Die Casting Process for Aluminum Powertrain and Structural Components. Advanced Engineering Materials 2019, 21 (6), 1800105.
- [5] Dash, S S, Li, D J, Zeng, X Q, Chen, D L. Heterogeneous Microstructure and Deformation Behavior of an Automotive Grade Aluminum Alloy. Journal of Alloys and Compounds 2021, 870, 159413.
- [6] Yang, J, Liu, B, Shu, D, Yang, Q,et al. Vehicle Giga-Casting Al Alloys Technologies, Applications, and Beyond. Journal of Alloys and Compounds 2025, 1013, 178552.
- [7] Czerwinski, F. Current Trends in Automotive Lightweighting Strategies and Materials. Materials 2021, 14 (21), 6631.
- [8] Sun, J, Dong, X, Li, S, Yang, H,et al. Effects of Composition and Natural Ageing on Microstructure and Mechanical Properties of Al-Mg-Si Heat Treatment-Free Die-Cast Alloys Assisted with Machine Learning. Materials Today Communications 2025, 47, 113000.
- [9] Dong, X, Liu, Q, Han, W, Yang, H,et al. Intelligent Development of High Strength and Ductile Heat Treatment-Free Al-Si-Mg Alloys for Integrated Die Casting through the Machine Learning of Experimental Big Data. Journal of Alloys and Compounds 2025, 1021, 179769.

- [10] Hu, M, Sun, D, Zhu, M. Simulation of Gas Porosity Formation and Interaction with Dendrite and Eutectic Structures during Solidification of Al-Si Alloys. Materials & Design 2024, 241, 112977.
- [11] Li, X X, Yang, X H, Xue, C P, Wang, S,et al. Hydrogen Microporosity Evolution and Dendrite Growth during Long Solidification of Al-Cu-Li Alloys: Modeling and Experiment. Journal of Materials Processing Technology 2023, 321, 118135.
- [12] Kallas, M K. Multi-Directional Unibody Casting Machine for a Vehicle Frame and Associated Methods. US20190217380A1, July 18, 2019.
- [13] Duan, H Q, Han, Z Y, Wang, B. Research Progress on Non-Heat Treatment Die Casting AluminumAlloy for Automotive Structural Parts. Automobile Technology & Materia 2022, No. 05, 1 - 6.
- [14] Sigworth, G K, Donahue, R J. The Metallurgy of Aluminum Alloys for Structural High-Pressure Die Castings. Inter Metalcast 2021, 15 (3), 1031 1046.
- [15] Dash, S S, Chen, D. A Review on Processing Microstructure
 Property Relationships of Al-Si Alloys: Recent Advances in Deformation Behavior. Metals 2023, 13 (3), 609.
- [16] Lumley, R. The Development of High Strength and Ductility in High-Pressure Die-Cast Al-Si-Mg Alloys from Secondary Sources. JOM 2019, 71 (1), 382 – 390.
- [17] Luo, T R, Fan, Z Z, Hu, H X, Wang, J H,et al. Research Status and Development Trend of Integrated Die-Casting Aluminum Alloyfor New Energy Vehicles. Special Casting & Nonferrous Alloys 2023, 43 (11), 1472 - 1478.
- [18] Li, Q, Wang, J, Liu, X, Wang, B. Minimizing Detrimental Impacts of β -Fe in Al-Mg-Si Alloy by Combining Thermal and Compression Processes. Materials Characterization 2023, 198, 112752.
- [19] Jin, L, Liu, K, Chen, X G. Evolution of Fe-Rich Intermetallics in Al-Si-Cu 319 Cast Alloy with Various Fe, Mo, and Mn Contents. Metall Mater Trans B 2019, 50 (4), 1896 – 1907.
- [20] Seifeddine, S, Svensson, I L. The Influence of Fe and Mn Content and Cooling Rate on the Microstructure and Mechanical Properties of A380-Die Casting Alloys. Metallurgical Science and Tecnology 2009, 27 (1).
- [21] Alhawari, K S, Omar, M Z, Ghazali, M J, Salleh, M S, et al. Microstructural Evolution during Semisolid Processing of Al-Si-Cu Alloy with Different Mg Contents. Transactions of Nonferrous Metals Society of China 2017, 27 (7), 1483-1497.
- [22] Luo, A A, Sachdev, A K, Apelian, D. Alloy Development and Process Innovations for Light Metals Casting. Journal

- of Materials Processing Technology 2022, 306, 117606.
- [23] Salleh, M S, Omar, M Z. Influence of Cu Content on Microstructure and Mechanical Properties of Thixoformed Al-Si-Cu-Mg Alloys. Transactions of Nonferrous Metals Society of China 2015, 25 (11), 3523 - 3538.
- [24] Hu, R, Guo, C, Ma, M. A Study on High Strength, High Plasticity, Non-Heat Treated Die-Cast Aluminum Alloy. Materials 2022, 15 (1), 295.
- [25] Li, Q, Wang, J S, Xue, C P, Miao, Y S,et al. Effects of Sr on Fe-Rich Intermetallics in Recycled Al-Si-Cu Alloys. J Mater Sci 2024, 59 (25), 11572-11595.
- [26] Hu, C, Zhu, H, Wang, Y, Xia, C,et al. Microstructure Features and Mechanical Properties of Non-Heat Treated HPDC Al9Si0.6Mn - TiB2 Alloys. Journal of Materials Research and Technology 2023, 27, 2117-2131.
- [27] Hartlieb, M. Aluminum Alloys for Structural Die Casting. Die casting engineer 2013, 57 (3), 40-43.
- [28] Hartlieb, M. High Integrity Diecasting for Structural Applications; Worcester Polytechnic Institute (WPI), MA, 2013; Vol. 12.
- [29] Sadayappan, K, Birsan, G, Caron, F,others. High Pressure Die Casting Aluminum Alloys for Automotive Structural Applications. Die Cast Eng 2017, 6 (61), 8-18.
- [30] STUCKI, J, PATTINSON, G, HAMILL, Q, PRABHU, A,et al. DIE CAST ALUMINUM ALLOYS FOR STRUCTURAL COMPONENTS. WO2021150604(A1), 2021.
- [31] Guo, J H, Ye, Y P, Zhao, Y B, Zhao, W B, et al. Aluminum Alloy Structural Member Material and Preparation Method Thereof. CN202010018461.7, 2020.
- [32] Zhang, J C, Zhong, G, Liu, J D, Gui, X H,et al. As-Cast High-Strength and High-Toughness Die-Cast Aluminum Alloy and Its Preparation Method. CN202210418545.9, 2023.
- [33] Xiong, S M, Tong, G D, Jiao, X Y, Wang, J,et al. As Cast High Toughness Die Cast Al-Si Alloy, Its Preparation Method and Applications. CN201910449860.6, November 10, 2020
- [34] Peng, L M, Yuan, L Y, Yang, L, Xiao, G,et al. Preparation Method for a Non-heat-treated Reinforced High Strength, High Toughness Die Cast Al-Si Alloy. CN202210038 413.3, October 14, 2022.
- [35] Huang, H, Zhu, Y, Yan, F, Lin, Y,et al. An As-Cast High Strength and High Toughness Die Cast Aluminum Alloy, and Its Method of Preparation and Product. CN202310223 358.X, April 14, 2023.
- [36] Wu, X X, Cheng, T J, Zhang, X M, Yin, R. A Die Cast Aluminum Alloy without Heat Treatment, Its Preparation Method and Applications. CN202310604165.9, June 23, 2023.
- [37] Ren, Y H, Xia, C Y, Wei, J Q, Wang, B X,et al. A Heat

- Treatment Free High Vacuum Die Cast Aluminum Alloy and Its Preparation Method. CN202310751635.4, September 19, 2023.
- [38] Zhan, H Y, Zeng, G, Wang, Q G, Wang, C J,et al. Unified Casting (UniCast) Aluminum Alloy—a Sustainable and Low-Carbon Materials Solution for Vehicle Lightweighting. Journal of Materials Science & Technology 2023, 154, 251 268.
- [39] Huang, H, Dan, Z X, Zhu, Y, Lin, Y,et al. Research Status and Development Trends of Heat-Free Aluminum Alloy by IntegratedDie Casting. SPECIAL CASTING & NONFERROUS ALLOYS 2024, 44 (08), 1054 - 1061.
- [40] Tong, G D, Xiong, S M, Jiao, X Y, Zhang, Y F,et al. High Strength and High Toughness Al – Si Alloy, Die Casting Preparation Method, and Application. CN202010270476.2, July 28, 2020.
- [41]Xiong, S M, Zhang, Y F, Liu, Y X, Wang, C G,et al. High-Strength and Tough Al - Si Die Casting Alloy and Its Manufacturing Process and Application. CN202210966123.5, November 8, 2022.
- [42]Yuan, L-Y, Han, P-W, Asghar, G, Liu, B-L,et al.

 Development of High Strength and Toughness

 Non-Heated Al Mg Si Alloys for High-Pressure

 Die-Casting. Acta Metall. Sin. (Engl. Lett.) 2021, 34 (6),

 845 860
- [43] Peng, L M, Yuan, L Y, Liu, B L, Wang, Q D,et al. High-Strength and High-Toughness Heat Treatment-Free Die-Cast Al - Mg - Si Alloy and Its Preparation Method. CN201810815626.6, December 6, 2019.
- [44] Wang, Y, Cao, L, Wu, X, Lin, X,et al. Multi-Alloying Effect of Ti, Mn, Cr, Zr, Er on the Cast Al-Zn-Mg-Cu Alloys. Materials Characterization 2023, 201, 112984.
- [45] Zhu, X, Blake, P, Dou, K, Ji, S. Strengthening Die-Cast Al-Mg and Al-Mg-Mn Alloys with Fe as a Beneficial Element. Materials Science and Engineering: A 2018, 732, 240 250.
- [46] Karamouz, M, Jesmani, S M. Hybrid Modification of Microstructure and Tensile Properties of A319 Alloy by Heat Treatment and Be Addition. JOM 2024, 76 (12), 7002 - 7010.
- [47] Tan, Y X, Ma, J H, Zhao, H D, Xu, Q Y. Progress in Integrated Die Casting of Aluminum Alloys. Aeronautical Manufacturing Technology 2024, 67 (14), 66 75.
- [48] Zhang, P, Li, Z, Liu, B, Ding, W,et al. Improved Tensile Properties of a New Aluminum Alloy for High Pressure Die Casting. Materials Science and Engineering: A 2016, 651, 376 390.
- [49] Song, D F, Huang, S P, Zhou, N, Li, X T,et al. A Heat Treatment-Free, High Thermal Conductivity Die-Cast

- Aluminum Alloy, Its Preparation Method, and Applications. CN202210592113.X, July 15, 2022.
- [50] Li, D J, Wang, X Y, Zeng, X Q, Li, Z X,et al. A Heat Treatment–Free High-Strength and High-Toughness Die-Cast Aluminum Alloy and Its Preparation Method. CN202210646779.9, June 6, 2023.
- [51] Chen, X D, Zhang, X M. A Heat Treatment-Free Die-Cast Aluminum Alloy, Its Preparation Method, and Automotive Structural Applications. CN202311507895.3, February 20, 2024.
- [52] Wang, Z M, Wang, X B, Ma, H J, Zhang, C,et al. Die Cast Aluminum Alloy Material, Its Preparation Method, and Applications. CN202211413943.8, April 14, 2023.
- [53] Fiorese, E, Bonollo, F, Timelli, G, Arnberg, L, et al. New Classification of Defects and Imperfections for Aluminum Alloy Castings. Inter Metalcast 2015, 9 (1), 55–66.
- [54] Lee, P D, Chirazi, A, See, D. Modeling Microporosity in Aluminum-Silicon Alloys: A Review. Journal of Light Metals 2001, 1 (1), 15–30.
- [55] Avalle, M, Belingardi, G, Cavatorta, M P, Doglione, R. Casting Defects and Fatigue Strength of a Die Cast Aluminium Alloy: A Comparison between Standard Specimens and Production Components. International Journal of Fatigue 2002, 24 (1), 1–9.
- [56] Wan, Q, Zhao, H, Zou, C. Effect of Micro-Porosities on Fatigue Behavior in Aluminum Die Castings by 3D X-Ray Tomography Inspection. ISIJ international 2014, 54 (3), 511–515.
- [57] Niu, X P, Hu, B H, Pinwill, I, Li, H. Vacuum Assisted High Pressure Die Casting of Aluminium Alloys. Journal of Materials Processing Technology 2000, 105 (1), 119–127.
- [58] Dybowski, B, Kiełbus, A, Poloczek, Ł. Effects of Die-Casting Defects on the Blister Formation in High-Pressure Die-Casting Aluminum Structural Components. Engineering Failure Analysis 2023, 150, 107223.
- [59] Matisková, D, Gašpar, Š, Mura, L. Thermal Factors of Die Casting and Their Impact on the Service Life of Moulds and the Quality of Castings. Acta Polytechnica Hungarica 2013, 10 (3), 65–78.
- [60] Niu, Z, Liu, G, Li, T, Ji, S. Effect of High Pressure

- Die Casting on the Castability, Defects and Mechanical Properties of Aluminium Alloys in Extra-Large Thin-Wall Castings. Journal of Materials Processing Technology 2022, 303, 117525.
- [61] Lalpoor, M, Eskin, D G, ten Brink, G, Katgerman, L. Microstructural Features of Intergranular Brittle Fracture and Cold Cracking in High Strength Aluminum Alloys. Materials Science and Engineering: A 2010, 527 (7), 1828–1834.
- [62] Suyitno, Eskin, D G, Katgerman, L. Structure Observations Related to Hot Tearing of Al-Cu Billets Produced by Direct-Chill Casting. Materials Science and Engineering: A 2006, 420 (1), 1-7.
- [63] Song, H, Zhang, L, Sun, J, Zhang, D,et al. Research on the Formation Mechanism and Fracture Behavior of Bifilm Defects. Journal of Materials Research and Technology 2023, 26, 6919–6927.
- [64] Campbell, J. An Overview of the Effects of Bifilms on the Structure and Properties of Cast Alloys. Metallurgical and Materials Transactions B 2006, 37 (6), 857–863.
- [65] El-Sayed, M A, Hassanin, H, Essa, K. Bifilm Defects and Porosity in Al Cast Alloys. Int J Adv Manuf Technol 2016, 86 (5), 1173–1179.
- [66] Dong, J, Jiang, J, Wang, Y, Qin, T,et al. Research on Numerical Simulation and Integrated Die Casting Process of Large Complex Thin-Walled Aluminum Alloy Automobile Rear Floor. Results in Engineering 2025, 26, 105399.
- [67] Kim, R C, Hong, K R, Yang, J Y, Yang, W C. High-Pressure Die Casting Process Optimization for Improving Shrinkage Porosity and Air Entrainment in Carburetor Housing with Aluminum Alloy Using Taguchi-Based ProCAST Simulation and MADM-Based Overall Quality Index. Int J Adv Manuf Technol 2024, 132 (1), 893–906.
- [68] Xu, H, Liu, W, Wang, Y, Ma, S,et al. Control and Optimization of Defects in Die Casting of Complicated Right Crankcase Cover. Journal of Materials Research and Technology 2024, 33, 2831–2840.
- [69] Li, Z Y, Wu, X L, Miao, Y S, Xue, C P,et al. Effects of Low-Pressure Casting Processes on Shrinkage

- PorosityFormation in Al Alloys. FOUNDRY TECHNOLOGY 2024, 45 (02), 163–172.
- [70] Shahane, S, Aluru, N, Ferreira, P, Kapoor, S G, et al. Optimization of Solidification in Die Casting Using Numerical Simulations and Machine Learning. Journal of Manufacturing Processes 2020, 51, 130–141.
- [71] Yang, J, Liu, B, Shu, D, Li, H,et al. Effect of Casting Pressure on Porosity, Microstructure, and Mechanical Properties of Large Die Casting Aluminum Alloy Parts. International Journal of Metalcasting 2025, 1–15.
- [72] Cao, H, Wang, C, Shan, Q, Che, J,et al. Kinetic Analysis of Pore Formation in Die-Cast Metals and Influence of Absolute Pressure on Porosity. Vacuum 2019, 168, 108828.
- [73] Szalva, P, Orbulov, I N. The Effect of Vacuum on the Mechanical Properties of Die Cast Aluminum AlSi9Cu3(Fe) Alloy. International Journal of Metalcasting 2019, 13 (4), 853–864.
- [74] Yang, J, Liu, B, Shu, D, Li, H,et al. Effect of Ultra Vacuum Assisted High Pressure Die Casting on the Mechanical Properties of Al-Si-Mn-Mg Alloy. Journal of Alloys and Compounds 2025, 1026, 180531.
- [75] Dou, K, Lordan, E, Zhang, Y, Jacot, A,et al. A Novel Approach to Optimize Mechanical Properties for Aluminium Alloy in High Pressure Die Casting (HPDC) Process Combining Experiment and Modelling. Journal of Materials Processing Technology 2021, 296, 117193.
- [76] Kim, H H, Lee, S M, Kang, C G. Reduction in Liquid Segregation and Microstructure Improvement in a Semisolid Die Casting Process by Varying Injection Velocity. Metall Mater Trans B 2011, 42 (1), 156–170.
- [77] Dong, G, Li, S, Ma, S, Zhang, D,et al. Process Optimization of A356 Aluminum Alloy Wheel Hub Fabricated by Low-Pressure Die Casting with Simulation and Experimental Coupling Methods. Journal of Materials Research and Technology 2023, 24, 3118–3132.
- [78] Lee, C D. Effects of Microporosity on Tensile Properties of A356 Aluminum Alloy. Materials



- Science and Engineering: A 2007, 464 (1–2), 249–254.
- [79] Lordan, E, Lazaro-Nebreda, J, Zhang, Y, Dou, K,et al. On the Relationship between Internal Porosity and the Tensile Ductility of Aluminium Alloy Die-Castings. Materials Science and Engineering: A 2020, 778, 139107.
- [80] Kong, D, Sun, D-Z, Yang, B, Qiao, H,et al. Characterization and Modeling of Damage Behavior of a Casting Aluminum Wheel Considering Inhomogeneity of Microstructure and Microdefects. Engineering Failure Analysis 2023, 145, 107018.
- [81] Zhang, Y, Tan, W, Zheng, J, Li, W, et al. Quantitative Analysis of 3D Pore Characteristics Effect on the Ductility of HPDC Al–10Si-0.3 Mg Alloy through X-Ray Tomography. Journal of Materials Research and Technology 2023, 26, 8079–8096.
- [82] Zhang, Y, Xue, C, Wang, J, Yang, X,et al. Quantifying the Effects of Hydrogen Concentration and Cooling Rates on Porosity Formation in Al–Li Alloys. Journal of Materials Research and Technology 2023, 26, 1938–1954.
- [83] Teng, X, Mae, H, Bai, Y, Wierzbicki, T. Pore Size and Fracture Ductility of Aluminum Low Pressure Die Casting. Engineering Fracture Mechanics 2009, 76 (8), 983–996.
- [84] Liu, R, Zheng, J, Godlewski, L, Zindel, J,et al. Influence of Pore Characteristics and Eutectic Particles on the Tensile Properties of Al–Si–Mn–Mg High Pressure Die Casting Alloy. Materials Science and Engineering: A 2020, 783, 139280.
- [85] Zhang, Y, Lordan, E, Dou, K, Wang, S,et al. Influence of Porosity Characteristics on the Variability in Mechanical Properties of High Pressure Die Casting (HPDC) AlSi7MgMn Alloys. Journal of Manufacturing Processes 2020, 56, 500–509.
- [86] Tebaldini, M, Petrogalli, C, Donzella, G, La Vecchia, G M. Estimation of Fatigue Limit of a A356-T6 Automotive Wheel in Presence of Defects. Procedia Structural Integrity 2017, 7, 521–529.
- [87] Ren, P, Huang, W, Zuo, Z, Li, D,et al. High Cycle Fatigue Analysis and Modelling of Cast Al–Si

- Alloys Extracted from Cylinder Heads Considering Microstructure Characteristics. Journal of Materials Research and Technology 2022, 19, 3004–3017.
- [88] Streck, S, Wiege, T, Dietrich, S, Herger, R,et al. Influence of Pores on the Lifetime of Die Cast Aluminium Alloys Studied by Fracture Mechanics and X-Ray Computed Tomography. Engineering Fracture Mechanics 2023, 284, 109243.
- [89] Yan, K, Huang, W, Zuo, Z, Ren, P,et al. Microstructure Based Analysis and Predictive Modeling of Cast Al7Si1.5Cu0.4Mg Alloy Mechanical Properties. Materials Today Communications 2022, 30, 103102.
- [90] Li, Z, Jing, Y, Guo, H, Sun, X,et al. Study of 3D Pores and Its Relationship with Crack Initiation Factors of Aluminum Alloy Die Castings. Metall Mater Trans B 2019, 50 (3), 1204–1212.
- [91] Afroz, L, Inverarity, S B, Qian, M, Easton, M, et al. Analysing the Effect of Defects on Stress Concentration and Fatigue Life of L-PBF AlSi10Mg Alloy Using Finite Element Modelling. Prog Addit Manuf 2024, 9 (2), 341–359.
- [92] Nicoletto, G, Konečná, R, Fintova, S. Characterization of Microshrinkage Casting Defects of Al–Si Alloys by X-Ray Computed Tomography and Metallography. International Journal of Fatigue 2012, 41, 39–46.
- [93] Le, V-D, Saintier, N, Morel, F, Bellett, D,et al. Investigation of the Effect of Porosity on the High Cycle Fatigue Behaviour of Cast Al-Si Alloy by X-Ray Micro-Tomography. International Journal of Fatigue 2018, 106, 24–37.
- [94] Chaijaruwanich, A, Lee, P D, Dashwood, R J, Youssef, Y M, et al. Evolution of Pore Morphology and Distribution during the Homogenization of Direct Chill Cast Al–Mg Alloys. Acta Materialia 2007, 55 (1), 285–293.
- [95] Hou, Q, Wang, J, Miao, Y, Li, X,et al. Predicting the Effect of Cooling Rates and Initial Hydrogen Concentrations on Porosity Formation in Al-Si Castings. Materials Genome Engineering Advances 2024, 2 (3), e37.
- [96] Atwood, R C, Lee, P D. Simulation of the Three-Dimensional Morphology of Solidification

- Porosity in an Aluminium–Silicon Alloy. Acta Materialia 2003, 51 (18), 5447–5466.
- [97] Yi, J Z, Lee, P D, Lindley, T C, Fukui, T. Statistical Modeling of Microstructure and Defect Population Effects on the Fatigue Performance of Cast A356-T6 Automotive Components. Materials Science and Engineering: A 2006, 432 (1–2), 59–68.
- [98] Li, P, Lee, P D, Maijer, D M, Lindley, T C. Quantification of the Interaction within Defect Populations on Fatigue Behavior in an Aluminum Alloy. Acta Materialia 2009, 57 (12), 3539–3548.
- [99] Serrano-Munoz, I, Buffiere, J-Y, Mokso, R, Verdu, C,et al. Location, Location & Size: Defects Close to Surfaces Dominate Fatigue Crack Initiation. Sci Rep 2017, 7 (1), 45239.
- [100]Szalva, P, Orbulov, I N. Fatigue Testing and Non-Destructive Characterization of AlSi9Cu3(Fe) Die Cast Specimens by Computer Tomography. Fatigue & Fracture of Engineering Materials & Structures 2020, 43 (9), 1949–1958.
- [101] Toda, H, Masuda, S, Batres, R, Kobayashi, M, et al. Statistical Assessment of Fatigue Crack Initiation from Sub-Surface Hydrogen Micropores in High-Quality Die-Cast Aluminum. Acta Materialia 2011, 59 (12), 4990–4998.
- [102]Yang, J, Liu, B, Shu, D, Yang, Q,et al. Local Stress/Strain Field Analysis of Die-Casting Al Alloys via 3D Model Simulation with Realistic Defect Distribution and RVE Modelling. Engineering Failure Analysis 2025, 168, 109104.
- [103]Zhang, Y, Zheng, J, Shen, F, Han, W,et al. Analysis of Local Stress/Strain Fields in an HPDC AM60 Plate Containing Pores with Various Characteristics. Engineering Failure Analysis 2021, 127, 105503.
- [104]Miao, Y S, Li, Z Y, Wu, X L, Feng, S wei,et al. Identifying the Critical Micropores Characteristics for the Degradation of Mechanical Properties in Automotive Wheels. Journal of Materials Research and Technology 2025, 36, 8075–8087.
- [105]Wang, S H, Li, Z Y, Ma, X Y, Wu, X L,et al. Integrated Predictions of the Influence of Mesh Size, Casting Defects and SDAS on the Fatigue Life of Aluminum Alloy Wheels. Journal of Materials Research and Technology 2025, 35, 3956–3967.

- [106]Li, X X, Wang, J S, Yang, X H, Xue, C P,et al. Effect of Solid Solution Treatment on the Kinetics of Hydrogen Porosity Evolution and Mechanical Properties in Al-Cu-Li Alloys. Vacuum 2024, 224, 113157.
- [107]Li, X X, Wang, J S, Miao, Y S, Li, Q,et al. In-Situ Study on the Effect of Li Concentration on Hydrogen Microporosity Evolution in Al-Li Alloys by Synchrotron X-Ray Radiography. Journal of Alloys and Compounds 2024, 1008, 176810.
- [108]Li, X X, Wang, J S, Xue, C P, Miao, Y S,et al. In-Situ Observation of Hydrogen Microporosity Nucleation and Growth during Superheating of Al–Li Alloy. Materials Research Letters 2025, 1–9.
- [109] Wang, X, Xu, L, Zhao, L, Ren, W,et al. Machine Learning Method for Estimating the Defect-Related Mechanical Properties of Additive Manufactured Alloys. Engineering Fracture Mechanics 2023, 291, 109559.
- [110]Kazup, Á, Garami, A, Gácsi, Z. Prediction of the Tensile Properties of A356 Casted Alloy Based on the Pore Structure Using Machine Learning. Materials Science and Engineering: A 2025, 935, 148338.
- [111]Zhai, Q, Tang, R, Liu, Z, Zhu, P. A Novel Method for Predicting Mechanical Properties of Megacasting Alloy Based on the Modified GTN Model and Machine Learning. Engineering Failure Analysis 2025, 174, 109536.
- [112]Chen, S, Kaufmann, T. Development of Data-Driven Machine Learning Models for the Prediction of Casting Surface Defects. Metals 2022, 12 (1), 1.
- [113]Yang, D, Tan, Y, Liao, P, Jiang, D,et al. Investigation of the Synergistic Evolution of Mechanical Properties Governed by Composition-Process-Microstructure Coupling in Ultra-Long Flow Die-Cast Aluminum Alloys. Journal of Manufacturing Processes 2025, 145, 508-521.
- [114]Hou, Q, Wu, X, Li, Z, Feng, S,et al. Artificial Intelligence Enabled Microstructure Prediction in Al Alloy Castings. Journal of Materials Science & Technology 2026, 241, 21–34.

- [115]Yang, J, Liu, B, Shu, D, Yang, Q,et al. Data-Driven Analysis of the Process, Organization and Properties of Large-Size Complex Thin-Walled Die-Casting Aluminium Alloys. Engineering Applications of Artificial Intelligence 2025, 156, 111244.
- [116]Li, C, Han, X, Yao, C, Guo, Y,et al. A Novel Training-Free Approach to Efficiently Extracting Material Microstructures via Visual Large Model. Acta Materialia 2025, 290, 120962.
- [117]Wu, X, Wang, J, Zhao, Q. HDD-Net: Haar Dual Domain Network for Ring Artifacts Correction. IEEE Trans. Comput. Imaging 2025, 11, 399–409.
- [118]Ma, J le, Zhang, W C, Han, Z Q, Xu, Q Y,et al. An Explainable Deep Learning Model Based on Multi-Scale Microstructure Information for Establishing Composition–Microstructure–Property Relationship

- of Aluminum Alloys. Integrating Materials and Manufacturing Innovation 2024, 13 (3), 827–842.
- [119]Guru, M K, Bohlen, J, Aydin, R C, Khalifa, N B. Machine Learning Pipeline for Structure–Property Modeling in Mg-Alloys Using Microstructure and Texture Descriptors. Acta Materialia 2025, 295, 121132.
- [120]Ren, D, Wang, C, Wei, X, Lai, Q,et al. Building a Quantitative Composition-Microstructure-Property Relationship of Dual-Phase Steels via Multimodal Data Mining. Acta Materialia 2023, 252, 118954.
- [121]Stromme, E T, Henderson, H B, Sims, Z C, Kesler, M S,et al. Ageless Aluminum-Cerium-Based Alloys in High-Volume Die Casting for Improved Energy Efficiency. JOM 2018, 70 (6), 866–871.